2MIL

NASA TECHNICAL MEMORANDUM

NASA TM X-64830

AN INVESTIGATION OF CHATTER AND TOOL WEAR WHEN MACHINING TITANIUM

By Ian A. Sutherland
Process Engineering Laboratory

January 1974

NASA

George C. Marshall Space Flight Center
Marshall Space Flight Center, Alabama

MSFC - Form 3190 (Rev June 1971)

TECHNICAL REPORT STANDARD TITLE PAGE

1. REPORT NO.	2. GOVERNMENT ACCESSION NO.	3. RECIPIENT'S CATALOG NO.
NASA TM X-64830		

4. TITLE AND SUBTITLE	5. REPORT DATE
An Investigation of Chatter and Tool Wear When Machining Titanium	January 1974
	6. PERFORMING ORGANIZATION CODE
7. AUTHOR(S) Ian A. Sutherland	8. PERFORMING ORGANIZATION REPORT #
9. PERFORMING ORGANIZATION NAME AND ADDRESS George C. Marshall Space Flight Center Marshall Space Flight Center, Alabama 35812	10. WORK UNIT NO.
	11. CONTRACT OR GRANT NO.
	13. TYPE OF REPORT & PERIOD COVERED Technical Memorandum
12. SPONSORING AGENCY NAME AND ADDRESS National Aeronautics and Space Administration Washington, D.C. 20546	14. SPONSORING AGENCY CODE

15. SUPPLEMENTARY NOTES
Prepared by Process Engineering Laboratory, Science and Engineering. Dr. Sutherland authored this work while he held an NRC Resident Research Associateship at Marshall Space Flight Center.

16. ABSTRACT

The low thermal conductivity of titanium, together with the low contact area between chip and tool and the unusually high chip velocities, gives rise to high tool tip temperatures and accelerated tool wear. Machining speeds have to be considerably reduced to avoid these high temperatures with a consequential loss of productivity. Restoring this lost productivity involves increasing other machining variables, such as feed and depth-of-cut, and can lead to another machining problem — namely, machine tool instability — more commonly known as chatter.

The object of this work is to acquaint the reader with these problems, to examine the variables that may be encountered when machining a material like titanium, and to advise the machine tool user on how to maximize the output from the machines and tooling available to him.

Recommendations are made on ways of improving machining tolerances, reducing machine tool instability or chatter, and improving productivity. New tool materials, tool coatings, and coolants are reviewed and their relevance examined when machining titanium.

Finally this report can be used as a guide to the reader who is interested in setting up a program of machine tool research.

17. KEY WORDS	18. DISTRIBUTION STATEMENT
	Unclassified-unlimited C. K. Vanderlaan

19. SECURITY CLASSIF. (of this report)	20. SECURITY CLASSIF. (of this page)	21. NO. OF PAGES	22. PRICE
Unclassified	Unclassified	75	NTIS

MSFC - Form 3292 (Rev December 1972) For sale by National Technical Information Service, Springfield, Virginia 22151

ACKOWLEDGMENTS

This report resulted from work accomplished while the author held a National Research Council Resident Research Associateship. The author would like to thank the Associateship directors, Drs. Thomas H. Curry and Roland W. Kinney, and in particular the coordinator for the Associateship Program at Marshall Space Flight Center, Dr. George C. Bucher, for their encouragement and support.

The author wishes to express his thanks to the many people in the host laboratory, Process Engineering, who have offered continual support and faultless assistance, in particular the Electrical Development Branch for their instrumentation support, the Master Mechanics Branch for their continued support in numerous areas, and the Special Process Branch for their support on machining tests.

The author is indebted to Dr. Siebel, who in his capacity as scientific advisor, has been a source of endless inspiration and, as laboratory director, has provided every facility for this work to be carried out. Thanks also goes to Dr. Siebel's secretarial staff, their excellent services have contributed significantly to the production of this report.

TABLE OF CONTENTS

		Page
SECTION I.	INTRODUCTION	1
SECTION II.	DESCRIPTION	1
	A. Foreword	1
	B. Theory	3
	1. Static Cutting	3
	2. Dynamic Cutting	8
	3. Stability Analysis	11
	C. Apparatus and Equipment	13
	D. Test Procedure	15
	E. Static Cutting Tests	16
	1. Introduction	16
	2. Static Tests (Free Machining Material)	17
	3. Static Tests (Titanium)	17
	4. Machining Titanium Compared to a Free-Machining Material	21
	5. Material Properties	23
	6. Discussion of Results	24
	F. Dynamic Cutting Tests	25
	1. Previous Work	25
	2. Dynamic Tests (Free Machining Material)	26
	3. Dynamic Tests (Titanium)	32
	4. Discussion of Results	35
	G. The Effect of New Tool Materials and Surface Treatments on the Machining of Titanium	39
	H. The Effect of Tool Finish on Machining Tolerance and Tool Life	41
	1. Introduction	41
	2. Tool Grinding and Machining Test Procedures	42
	3. Results of Machining Force Tests	44
	4. Results of Tool Life Tests	44
	5. Discussion of Results	48

TABLE OF CONTENTS (Concluded)

Page

I. The Effectiveness of Different Coolant Techniques in Reducing Tool Temperature. 53
1. Experimental Apparatus and Monitoring Equipment 53
2. Results 54
3. Discussion of Results 54

SECTION III. CONCLUSIONS 56

APPENDIX. 58

REFERENCES 60

LIST OF ILLUSTRATIONS

Figure	Title	Page
1.	Tool force components	4
2.	Force diagram used for shear-plane model of cutting	6
3.	Wave cutting	9
4.	Monitoring equipment and tool control system — schematic	15
5.	Variation of machining forces with undeformed chip thickness for different rake angles	18
6.	Variation of machining forces with undeformed chip thickness for different rake angles	19
7.	The variation of tool nose force with rake angle when machining titanium	20
8.	Variation of shear force and normal force with length of shear plane for brass	22
9.	Variation of shear force and normal force with length of shear plane for titanium	22
10.	The effect of clearance angle (γ_m) on the Cutting Pressure in the Thrust Direction — Brass	27
11.	The effect of clearance angle on the phase lead of dynamic thrust force relative to tool motion — Brass	28
12.	The contract force showing: a) typical trace of the dynamic thrust force, b) schematic representation of how the contact force arises	29
13.	The effect of rake angle (α) on cutting pressure and θ_t	30
14.	The effect of flank land (l) on dynamic cutting pressure in the thrust direction — brass	31

LIST OF ILLUSTRATIONS (Continued)

Figure	Title	Page
15.	The variation of dynamic cutting pressure in the thrust direction with l^2/λ for different flank lands (l) and wavelengths (λ) — brass	33
16.	The effect of clearance angle (γm) on the cutting pressure in the thrust direction — titanium	34
17.	The variation of θ_t with $l/\gamma_m \lambda$ — titanium	35
18.	The effect of rake angle (α) on the dynamic cutting pressure in the thrust direction — titanium	36
19.	Effect of flank land (l) on dynamic cutting pressure in thrust direction — titanium	37
20.	The variation of dynamic cutting pressure in the thrust direction with l^2/λ for different flank land (l) and wavelengths (λ) — titanium	38
21.	Flank wear comparison of 5h and 7g titanium carbide grades and c-7 tungsten carbide grade against titanium carbide coated cemented tungsten carbide tool A	40
22.	A typical tool flank wear with time curve	43
23.	The variation of machining forces with undeformed chip thickness for different rake angles — using a lapped tool	45
24.	The variation of machining forces with chip thickness for a TiC coated tungsten carbide tool	47
25.	The effect of a) feed and b) speed on the stock removed during the life of a conventionally ground tool	49
26.	The effect of a) feed b) speed on the stock removed during the life of a lapped tool	50

LIST OF ILLUSTRATIONS (Concluded)

Figure	Title	Page
27.	The variation of tool life with rate of stock removal comparing conventionally ground tooling with lapped tooling	51
28.	The variation of stock removed during the life of the tool with the rate of stock removal — when machining titanium	52
29.	Temperature drop with distance from tool tip for different coolant techniques	55
30.	Flank wear land against time curves, with and without coolant	56

LIST OF TABLES

Table	Title	Page
1.	The Ratios of Static Cutting Pressure and Nose Force When Machining Titanium, as Compared to Brass.	21
2.	Material Properties of Titanium and Brass From Machining Tests	23
3.	Comparing the Material Properties Obtained From Machining Tests With Those From Static Compression Tests	24
4.	The Effect on Nose Force of Lapping the Tool	46
5.	Tool Nose Forces for a TiC Coated Tool Compared to Conventionally Ground or Lapped Tools	48

LIST OF SYMBOLS

Symbols	Definition
F	Friction force along rake face
F_c	Static force in cutting direction
F_N	Normal or compressive force perpendicular to the shear plane (static)
F_s	Shear force along shear plane (static)
F_t	Static force in thrust direction
g	Feed
k_q	Dynamic cutting pressure in the thrust direction
k_s	Static cutting pressure in cutting direction
k_t	Penetration coefficient
k_l	Dynamic cutting coefficient perpendicular to the cutting direction, after Tobias [15]
K^*	Penetration coefficient, after Tobias [15]
l_s	Length of shear plane
N	Normal force perpendicular to rake face (static)
P	Static force on nose region of tool
p	Dynamic force on flank of tool
p_c	Contact force on flank of tool
Q	Static force on rake face of tool
q	Dynamic force on rake face of tool

LIST OF SYMBOLS (Continued)

Symbols	Definition
R	Resultant static force of tool
R_t	Amplitude of dynamic force in the thrust direction
r	Resultant dynamic force on tool
S	Surface Cutting speed
S_N	Normal stress perpendicular to shear plane (static)
S_s	Shear stress along shear plane (static)
t_1	Undeformed chip thickness
t_2	Deformed chip thickness
T	Tool life
w	Width of cut
X	Amplitude of oscillating component of undeformed chip thickness
x	Distance measured in the direction of the mean cutting velocity
z_c	Number of simultaneously cutting edges (unity for turning) after Tobias [15]
α	Rake angle
γ_i	Instantaneous clearance angle
γ_m	Mean clearance angle
δ	Instantaneous slope of the surface being cut
θ_t	Phase lead of dynamic thrust force relative to tool motion or undeformed chip thickness variation

LIST OF SYMBOLS (Concluded)

Symbols	Definition
λ	Wavelength of undeformed chip thickness variation
ϕ	Shear angle
τ	Friction angle
	Suffixes
c	in the cutting direction
N	normal to shear plane
S	along shear plane
t	in the thrust direction

TECHNICAL MEMORADUM X-64830

AN INVESTIGATION OF CHATTER AND TOOL WEAR WHEN MACHINING TITANIUM

SECTION I. INTRODUCTION

The increase in use of titanium in the aerospace industry is one example of a trend in the industry towards the use of new light materials to withstand high temperatures, high stresses, or corrosive environments. The need for machining these materials has created major problems in machine-tool equipment and techniques. When compared with standard engineering materials, titanium alloys exhibit low thermal conductivity and specific heat properties. Together with the low contact areas between chip and tool and the unusually high chip velocities, these properties give rise to high tool tip temperatures and accelerated tool wear. In order to obtain any useful life from a tool, the cutting speed must be significantly reduced, resulting in longer manufacturing times and increased production costs.

Specific recommendations concerning feeds and speeds for use in machining high strength materials are found in many publications [1,2,3,4]. The objective of the work reported here is to acquaint the reader with some of the problems and variables that may be encountered when machining such a material and what the machine tool user can do to get maximum output from the tools that are available to him.

The material chosen for the tests was Ti-6A1-4V, a particularly "difficult-to-machine" material that is widely used in the aerospace industry. More information on the material — properties, advantage, and usage in the aerospace industry — can be obtained by referring to the Appendix.

SECTION II. DESCRIPTION

A. Foreword

There are a number of variables that affect the machining process. These can be placed in the following categories:

(i) Machine Tool — mass, stiffness, damping, natural frequencies, and orientation of principal axes of vibration.

(ii) Machining — speed, feed, depth-of-cut*, width-of-cut, type of machining process (i.e., milling, turning, etc.), and number of teeth in contact.

(iii) Cutting Tool — tool material, nose radius, rake, clearance and approach angles, and surface finish.

(iv) Workpiece Material — material properties (strength, ductility, thermal conductivity, etc.) and chip formation (continuous, discontinuous or segmented).

The purpose of machine tool research is to reach an understanding of the machining in order to assess and understand the important variables and then improve manufacturing efficiency either by user education or by automation.

Improvements in the last twenty years have led to stiffer machine tools with higher natural frequencies. Normally this means that higher metal removal rates are possible before instability or chatter occurs. Machine tool instability, commonly known as chatter, occurs due to the dynamic interaction between the cutting process and the machine tool structure, in that cutting forces cause deflections between the tool and the workpiece leading to changes in the chip geometry that again affect the cutting forces. In the aerospace industry, however, the requirement for high temperature alloys that are "difficult-to-machine" have meant that the advantages of improved machine tool performance have been largely outweighed, in terms of chatter, by the increased strength of the materials being machined. Chatter, therefore, can still be a problem in the aerospace industry. Although some form of stabilization at low machining speeds has been found [5], it is not completely understood and the variables affecting this stability have not yet been fully documented.

As already mentioned in the Introduction, aerospace materials require low machining and therefore productivity is reduced. In order to increase productivity, the values of the variables listed in (ii) above need to be increased. Increasing depth-of-cut, however, is like increasing the gain of the feedback loop and can lead to instability, whereas increasing feed can generate higher tool temperatures and accelerate tool wear. It becomes necessary therefore to optimize the machining variables such as speed, feed, and depth-of-cut by using the cutting tool variables listed in (iii) above. This solution is of particular interest to the machine tool user, since he has control of these variables.

* Depth-of-cut and width-of-cut are synonymous for turning

It is proposed, therefore, in this report to examine:

(a) Static cutting — to study the effect of the tool variables on machining forces, to minimize machining forces and reduce machining tolerances.

(b) Dynamic cutting — to examine the variables causing low speed stability so that chatter problems can be minimized.

(c) The cutting tool — to review modern cutting tool technology.

(d) Cutting tool performance — to examine the parameters affecting tool life and to optimize speeds and feeds to obtain the highest stock removal for a given tool life while maximizing the rate of metal removal.

(e) Tool temperature — examining ways of decreasing tool temperature by means of suitable coolants, so that tool life can be extended and productivity increased.

In cases (a) and (b) above, Ti-6A1-4V titanium was used and compared to a free machining material, such as 60-40 Brass. In this way, it can be known whether a particular variable is affected by the material or whether it is a function of the machining process itself.

A single point turning operation is used, as it is one of the simplest machining operations. However, any machining or cutting tool parameters found to be important when turning titanium can be applied to other machining operations, where allowances are made for the different cutting geometries.

In this report, therefore, it is hoped to establish the values of independent variables that will improve productivity and machining tolerances. Some of these variables will be applicable to the machining of any materials, whereas others will apply only to the machining of titanium. It is hoped, nevertheless, that the discussion of experimental technique and research procedure will assist others in their efforts to solve machining problems.

B. Theory

1. Static Cutting. One of the earliest models of chip formation for orthogonal cutting was proposed by Merchant [6]. He assumed that the metal sheared across a thin shear plane, from the tool tip to the junction of the chip and work surface ahead of the tool (Fig. 1).

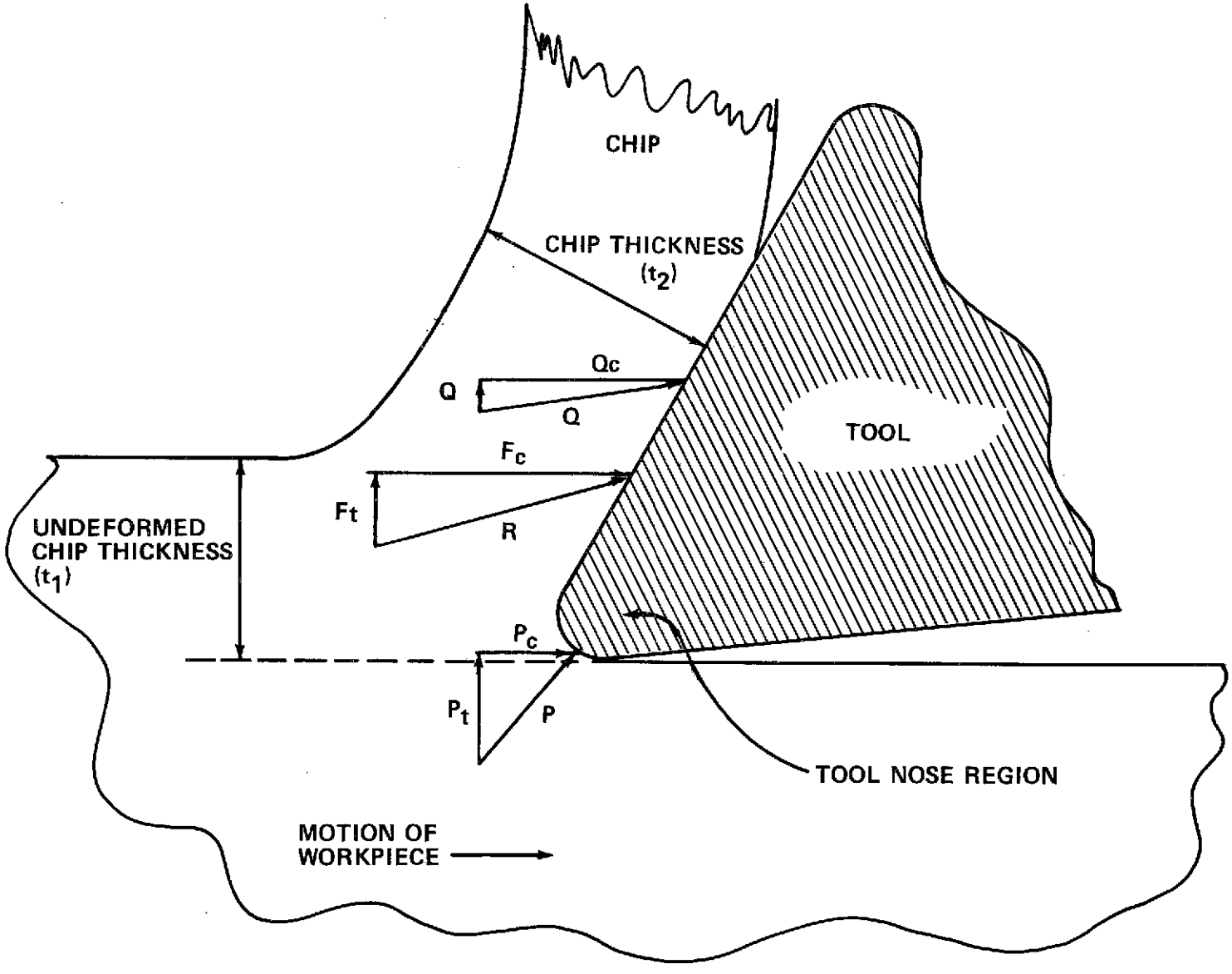

Figure 1. Tool force components.

Merchant's model is still used widely today, with a few modifications. It has now been established that the shear plane may be a shear zone or wedge with a finite width [7,8], but the thin shear plane is still considered a good approximation. The existence of a tool nose force, assumed negligible by Merchant, has been studied by Albrecht [9] and Wallace and Boothroyd [10]. They concluded that a nose force exists that is independent of the undeformed chip thickness and may be due to material deformation in the nose region of the tool. They further suggest that when evaluating such variables as shear stress, friction angle, and cutting pressure, that the nose force be subtracted from the measured force to give the "true" effect due to the chip acting on the rake face of the tool.

The resultant force R on the tool in Figure 1 can be considered as being the vector sum of the force on the tool nose (P) and the force in the rake face (Q), so that,

$$\bar{R} = \bar{P} + \bar{Q} \quad . \tag{1}$$

This cutting force (R) can be resolved in a number of ways as shown in Figure 2:

(a) In the cutting and thrust directions (F_c, F_t), parallel to and perpendicular to the direction of the cutting velocity.

(b) In the direction of the mean shear plane and perpendicular to it (F_s, F_N), where F_s is called the shear force and F_N the normal or compressive force.

(c) In a direction parallel and perpendicular to the rake face to give the rake face friction force (F) and normal force (N).

For steady state cutting and assuming a thin straight shear plane, the shear angle (ϕ) and the shear length (l_s) can be expressed from the geometry of Figure 2, as follows:

$$\phi = \tan^{-1} \left(\frac{t_1 \cdot \cos \alpha}{t_2 - t_1 \sin \alpha} \right) \tag{2}$$

and

$$l_s = t_1/\sin \phi \quad . \tag{3}$$

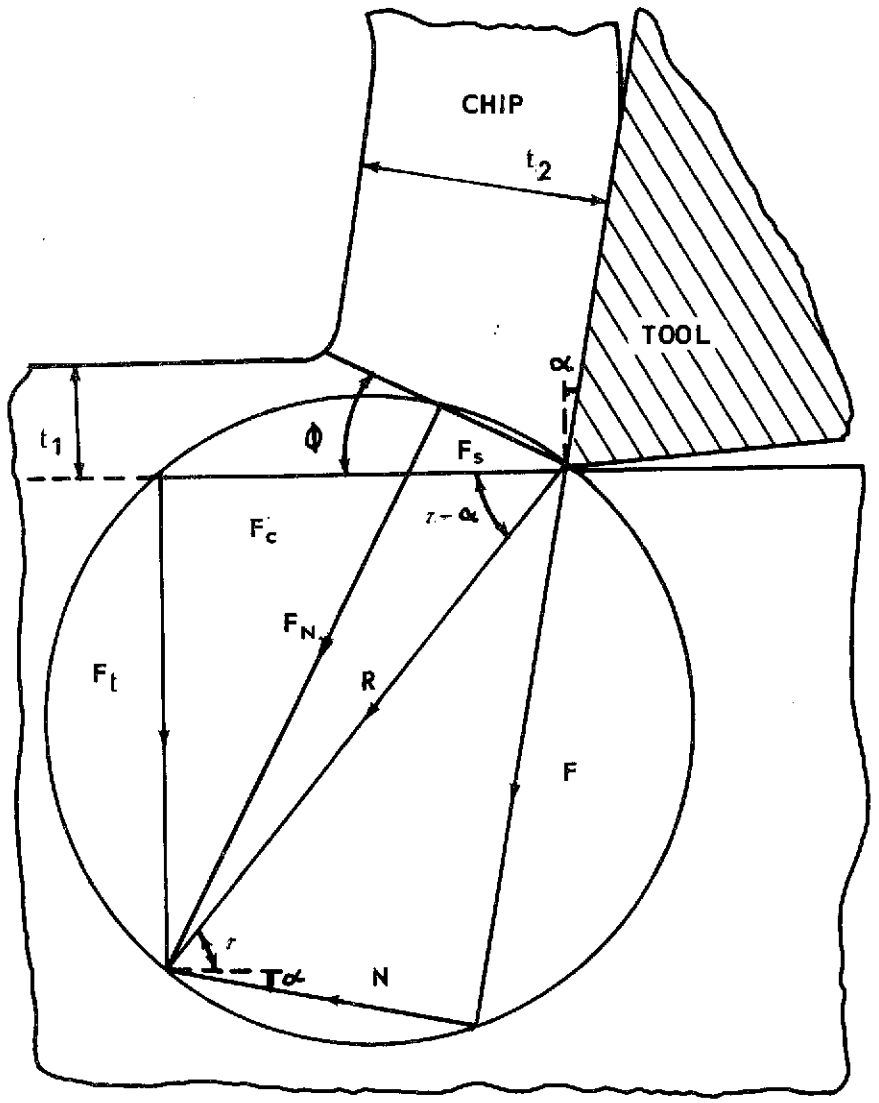

Figure 2. Force diagram used for shear-plane model of cutting.

If the forces in the cutting and thrust directions and the shear angle are known, then the forces acting on the shear plane can be calculated as

$$F_s = F_c \cos \phi - F_t \sin \phi \tag{4}$$

and

$$F_N = F_c \sin \phi + F_t \cos \phi \quad . \tag{5}$$

Now if F_c and F_t are plotted against chip thickness (t_1), then the friction angle (τ) and the static cutting pressure k_s can be expressed by

$$\tau = \alpha + \tan^{-1} \left(\frac{\Delta F_t}{\Delta t_1} \Big/ \frac{\Delta F_c}{\Delta t_1} \right) \quad , \tag{6}$$

where $\Delta F_t / \Delta t_1$ is the slope of the thrust force — undeformed chip thickness curve, and

$$k_s = \frac{1}{w} \cdot \frac{\Delta F_c}{\Delta t_1} \quad . \tag{7}$$

Now equations (6) and (7) are only valid if P in equation (1) is independent of undeformed chip thickness (t_1), an assumption justified extensively in [11], and the cutting force is proportional to undeformed chip thickness.

If F_s and F_N are plotted against the length of the shear plane (l_s), then the shear stress (S_s) and normal stress (S_N) can be claculated from the slope of the results as follows:

$$S_s = \frac{1}{w} \frac{\Delta F_s}{\Delta l_s} \tag{8}$$

and

$$S_N = \frac{1}{w} \frac{\Delta F_N}{\Delta l_s} \quad . \tag{9}$$

Alternatively, if these variables are found to vary with undeformed chip thickness, then the nose force (P) can be found by letting Q tend to zero in equation (1). With the components of P_c and P_t known, they can be subtracted from F_c and F_t to give only the chip/rake face force components Q_c and Q_t. Equations (6) through (9) could then be written using the actual corrected force values:

$$\tau = \alpha + \tan^{-1} [Q_t/Q_c] \quad , \tag{10}$$

$$k_s = Q_c/wt_1 \quad , \tag{11}$$

$$S_s = Q_s/wl_s \quad , \tag{12}$$

and

$$S_N = Q_n/wl_s \quad . \tag{13}$$

2. Dynamic Cutting. The type of oscillating cutting investigated is shown in Figure 3. The tool is oscillating with an amplitude X and wavelength λ, while machining an initially flat surface. The wavelength (λ) is a measure of the relative distance the tool travels with respect to the workpiece surface in one tool oscillation. Apparent oscillations of the shear plane due to the cutting velocity changes in direction are neglected, an assumption justified by Wallace and Andrew [12] in their work on wave-on-wave cutting.

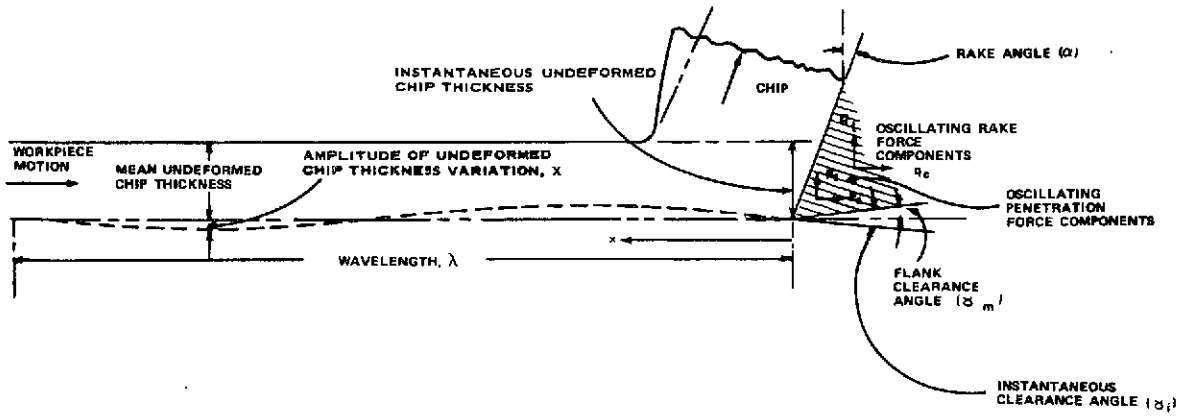

Figure 3. Wave cutting.

The oscillating component of undeformed chip thickness can be expressed by $X \sin (z\pi x/\lambda)$ and the oscillating force component acting on the rake face in the thrust direction can be expressed as:

$$q_t = k_q w X \sin (2\pi x/\lambda) \qquad (14)$$

where k_q is the dynamic cutting pressure in the thrust direction, and is a function of rake angle (α) and friction angle (τ).

Wallace and Andrew [12] considered the penetration force or flank force to be caused by a fluctuation of the effective clearance angle (γ_i). This has since been supported by Kegg [13] and Stewart [14]. Wallace and Kegg both attribute this force to some kind of contact between the flank and the workpiece, whereas Stewart and Sisson and Kegg in a later paper [5], assume that there is elastic deformation and subsequent recovery. If this is the case, then the extent of deformation can be given by $(\gamma_i - \gamma_m)/\gamma_m$ or (δ/γ_m) where γ_i is the instantaneous clearance angle, γ_m the mean clearance angle and δ the instantaneous slope of the surface being cut, provided $\delta < \gamma_m$ and δ is small. This latter term can be expressed as

$$\delta = \frac{2\pi X}{\lambda} \cos(2\pi x/\lambda) \quad . \tag{15}$$

The component of oscillating flank force in the thrust direction (P_t) can be considered as being a function of the extent of deformation (δ/γ_m), so that

$$p_t = k_t \cdot w \cdot \frac{2\pi X}{\lambda \gamma_m} \cos\left(\frac{2\pi x}{\lambda}\right) \quad , \tag{16}$$

where k_t is a coefficient dependent on the material, the cutting conditions, and the orientation of this oscillatory flank force. The force component can be called a quadrature force, as it leads the undeformed chip thickness oscillation with respect to time by a quarter of a wave length (i.e., a phase lead of 90°).

The total component of oscillation thrust force (r_t) is obtained by adding equations (14) and (16)

$$r_t = q_t + p_t \quad ;$$

therefore,

$$r_t = k_q w X \sin(2\pi x/\lambda) + \frac{k_t \cdot w \cdot 2\pi X}{\gamma_m \lambda} \cos(2\pi X/\lambda) \quad . \tag{17}$$

The amplitude of r_t will be given by

$$R_t = w X \sqrt{k_q^2 + \left(\frac{2\pi k_t}{\gamma_m \lambda}\right)^2} \quad . \tag{18}$$

The phase lead of R_t relative to the tool motion, with respect to time, will be

$$\theta_t = \tan^{-1}(2\pi k_t/\gamma_m \lambda k_q) \quad . \tag{19}$$

Now if $\delta > \gamma_m$, then rigid contact takes place between the tool and the workpiece and the above equations may not be valid. Tool/workpiece contact will occur when

$$\delta \max \geq \gamma_m \quad . \tag{20}$$

Substituting the maximum value of δ from equation (15) gives

$$\frac{1}{\gamma_m \lambda} = \frac{1}{2\pi X} \quad , \tag{21}$$

or, if γ_m is expressed in degrees, equation (21) becomes

$$\frac{1}{\gamma_m \lambda} = \frac{1}{360X} \quad . \tag{22}$$

If δ is large, then $\tan \delta$ will have to be considered instead of δ in equations (15), (21), and (22).

3. Stability Analysis. A stability analysis of the turning operation will not be discussed in great detail. Tobias [15] describes machine tool stability analysis for a number of machining operations. He concludes that two force components are predominant in affecting stability — namely, (i) an oscillatory force component on the tool rake face caused by the chip thickness variation effect, and (ii) an oscillatory force component caused by contact between the flank of the tool and the work piece, that he calls the penetration effect.

The first component may lead to instability in certain circumstances, while the second has so far always yielded a stabilizing influence. He examines two types of chatter: Type A, arising out of relative tool/workpiece flexibility perpendicular to the cutting velocity vector and Type B, from flexibility in the direction of the cutting velocity vector. Only Type A will be considered here, as it occurs most commonly in practice.

He finds the factors affecting stability most are $z_c k_1/\lambda$ and $z_c K^*/\lambda$. He defines z_c as the number of simultaneously cutting edges (unity for turning), k as the dynamic cutting coefficient perpendicular to the cutting direction for

Type A chatter, K* as the penetration coefficient, and λ as a stiffness term for the machine tool structure. He concludes that k_1 should be as small as possible, while λ and K* should be as large as possible for maximum stability.

The dynamic cutting coefficient (k_1) and penetration coefficient (K*), as used by Tobias, can be obtained from equations (14) and (16), whereby

$$k_1 = \frac{|q_t|}{X} = w\,k_q \quad , \text{ and} \tag{23}$$

$$K^* = \frac{|p_t|}{X} = \frac{2\pi w\,k_t}{\lambda\gamma m} \quad . \tag{24}$$

For maximum stability, width of cut, w, and dynamic cutting pressure, k_q, in equation (23) should be small. k_q is a function of sin $(\tau-\alpha)$, so that arranging for the friction angle (τ) to equal the rake angle (α) will minimize (k_q).

For maximum added damping due to the penetration coefficient K*, and consequently maximum stability, then k_t in equation (24) should be large and the wavelength, λ, and clearance angle, γ_m, should be small.

When measuring the dynamic cutting forces in the thrust direction, it is not possible to distinguish between the in-phase and quadrature forces, q_t and P_t. Instead, the amplitude of the dynamic cutting pressure in the thrust direction, R_t/wX, in equation (18), and the phase between this pressure and tool motion, θt in equation (19), are measured. It is possible, however, by plotting these quantities against the inverse of wavelength, $1/\lambda$, to calculate values of the in-phase and quadrature coefficients, k_q and k_t. The in-phase coefficient k_q is found from the intercept with the $1/\lambda = 0$ axis and the quadrature coefficient k_t is found by curve fitting. The amplitude of the in-phase component of thrust force in equation (14) is constant for a given width-of-cut, w, and vibration amplitude, X, and is expressed by k_q wX. The

amplitude of the quadrature component of thrust force in equation (16) for a given width-of-cut, w, and vibration amplitude, X, is still dependent on $1/\gamma_m\lambda$. A plot of R_t/wX and θ_t against $1/\lambda$ or $1/\gamma_m\lambda$ should show that the dynamic cutting pressure increases with $1/\lambda$ and that θ_t tends towards 90 degrees as the ratio $2\pi k_t/\gamma_m\lambda k_q$ becomes infinite in equation (19). This will be a result of the quadrature force P_t becoming large compared to the in-phase force q_t.

C. APPARATUS AND EQUIPMENT

A Monarch Lathe, Model 62, was used for the machining tests. Dynamic acceptance tests on the machine tool structure indicated that it was adequately stiff with a 0.15-m (6-in.) diameter workpiece, except for the tail stock that required the additional support of a steady. The structure was two orders of magnitude stiffer than the designed compressive stiffness of the tooling assembly. The workpiece used for all machining tests was mounted in a 400-mm (16-inch), 4-jaw chuck and supported by a dead center. Each workpiece was machined from the same batch of material with a 12.2-mm ($\frac{1}{2}$-in.) pitch square thread, 25.4-mm (1-in.) deep and with a width determined by the material used. In general, the width was 6.25mm (0.250 in.) for brass and 1.88mm (0.075 in.) for titanium. Undeformed chip thicknesses were kept below 10 percent of these values so that edge effects were minimized. The threaded length of the workpiece was approximately ten inches long, so that one machining run machined about 10 meters of material in 20 revolutions of the workpiece. The workpiece was designed in this way so that dynamic cutting tests could be arranged to (a) Machine a fresh workpiece surface with a vibrating tool — wave producing, and (b) Machine away a sinusoidal surface with a stationary tool — wave removing.

Since the workpiece thread, that was machined away during the cutting tests, has a 1.5 deg helix, the cutting tool was angled at 1.5 deg to the vertical so that there was no cutting velocity parallel to the cutting edge. Only orthogonal machining was examined, so that the machining process was only in one plane. This meant that a two-component force dynamometer could be used to measure the machining forces, namely one component in the cutting direction, parallel to the cutting velocity, and the other in the thrust direction, perpendicular to the cutting velocity.

The force dynamometer was designed to measure the cutting forces directly in the cutting and thrust directions. The tool control system was designed to either vibrate the tool in a sinusoidal manner, despite the machining forces acting on the tool, or to hold the tool stationary. A dc control

system as well as an ac control system were developed so that both static and dynamic stiffness was supplied to the tool. Both the force dynamometer and tool control system are described in more detail in an earlier report by the author [16].

The spindle rotational speed was monitored using an acoustic technique to pick up 60 pulses per revolution of the spindle. These pulses were input to a digital voltmeter to give a direct readout of spindle revolutions per minute.

The cross-slide position was monitored, using a linear voltage displacement transducer (LVDT). In this way, the depth of cut or undeformed chip thickness could be measured to within ± 0.0025mm (0.0001 inches) — an improvement factor of 10 over the normal cross-slide scale.

The tool displacement was detected by a strain gage on the flexible part of the dynamometer housing. The strain instrumentation consisted of an active and passive gage, which were wired in the same way as the force dynamometer strain gages described in [16]. Each strain gage bridge could be zeroed before testing began. Drift was found to be negligible.

The cutting force, thrust force, and displacement signals coming from the bridge circuitry were connected via operational amplifiers to an Ampex 14 channel tape recorder set up for loop operation (Fig. 4). The operational amplifiers served to attenuate the signals to the tape recorder if they became too large. The loop length could be varied to last between 3.75 to 30 seconds per loop, and would be chosen, with respect to the workpiece rotational speed, to record at least five revolutions of the workpiece. The tape recorder could be switched from record to replay by a microswitch mounted on the machine tool. In this way, the recording could be stopped before run-out of the cutter.

A digital voltmeter was used to monitor nearly all of the transducer signals before and after recording them on the tape recorder. It had the capability of switching to any signal, as shown in Figure 4. A Honeywell Visicorder was used to obtain a permanent record of each test, as the tape would re-record every machining test. When frequencies became too high for the Visicorder to record effectively, a photograph would be taken from an oscilloscope display. For the dynamic machining tests, the phase between any two signals could be obtained either (a) graphically from the visicorder plots, (b) graphically from a photograph taken from the oscilloscope, or (c) by direct measurement, using a phase meter.

Generally, the last method was preferred, since it was more accurate. However, in the event of the occurrence of non-linearity, graphical methods were employed.

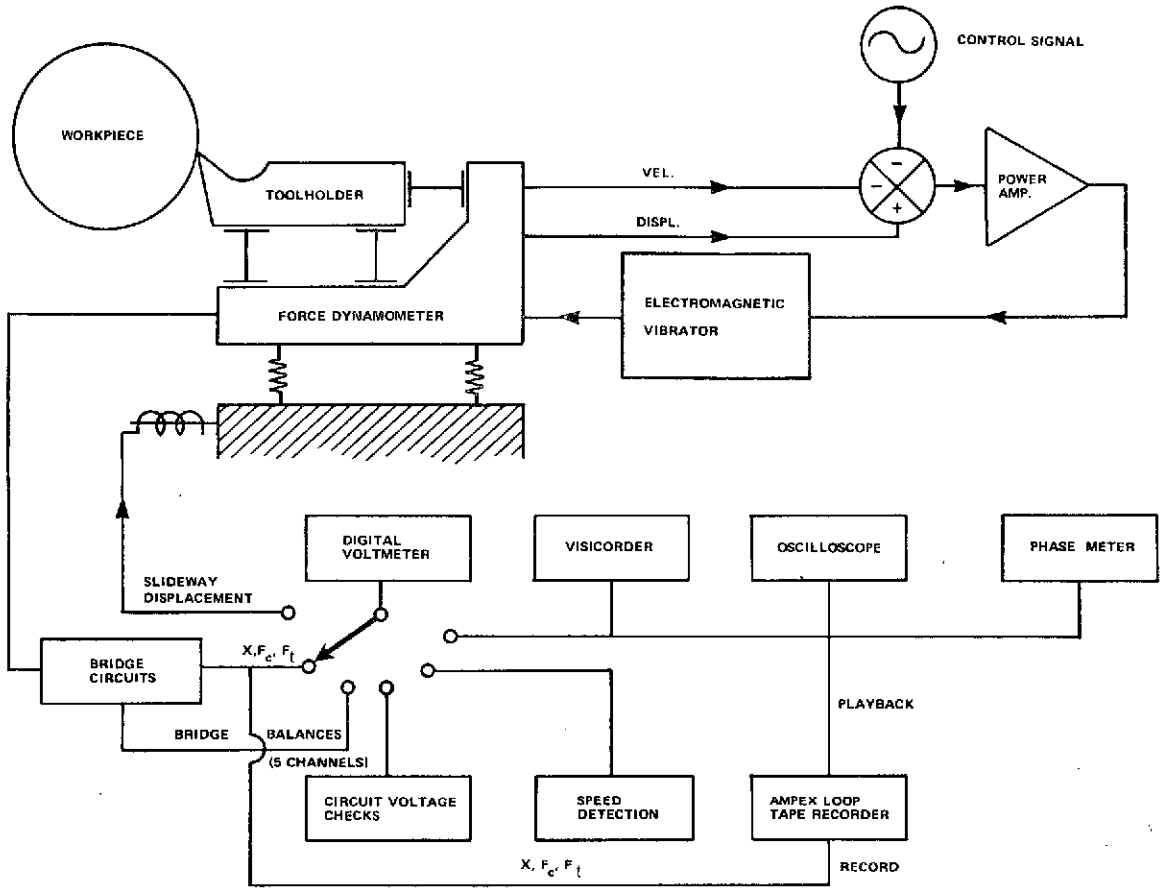

Figure 4. Monitoring equipment and tool control system — schematic.

D. Test Procedure

The tools used for all machining tests were the same grade of carbide and were ground with a 250-grit diamond wheel parallel to the cutting edge. The finish on the flank and rake face of each tool was maintained to within 0.38 to 0.50 micrometers (15 to 20 microinches) and the cutting edge was inspected before use for cracking or chipping. The tool angles were measured on a shadowgraph before the tool was mounted in the tool holder. The height of the tool above the centerline of the workpiece was measured for each tool and the effective rake and clearance angles were calculated. The tool was run-in until consistent machining conditions occurred. This consisted of machining approximately 30 meters (100 feet) of material to remove the initial sharpness of the cutter.

The tool control system was then set for either a sinusoidally oscillating or a stationary tool. If the tool was expected to oscillate, then the frequency and amplitude would be set at this stage.

The tape recorder would then be placed in a "record" mode and zero readings taken for force and displacement. These would be taken electrically, using a digital volt meter (DVM), and recorded graphically on ultra violet sensitive paper, using the visicorder.

The lathe rotational speed would be selected and the slide way set to give the appropriate undeformed chip thickness. The coordinates of the cross-slide would be noted from the LVDT reading on the DVM.

The tape recorder was arranged to switch from record to reproduce about two feet before the end of the cut, so that no "run out" effects were recorded. The data from the tape was then analyzed electrically, using either the DVM for oscillating and mean components of force and amplitude or the phase meter to measure the phase between two oscillating waveforms. The data was also recorded on the visicorder. If frequencies above 200 Hz were being used, then the displacement and force traces could be played back through an oscilloscope and photographed. The paper speed on the visicorder limited its use to recordings below 200 Hz.

After each machining run, the deformed chips would be collected and labeled and their thickness measured, using a tool makers microscope.

The cycle of machining tests would then be repeated until the tool had machined 150 meters, after which it would be reground. The tool showed no signs of wear with this usage.

E. Static Cutting Tests

1. Introduction. Static cutting tests are a useful indication of how a material behaves when it is machined, how machinability variations can be detected from one material to another, and how the optimum machining geometry is indicated for a given material.

The object of the following tests is to examine the machinability of titanium (Ti-6Al-4V) as compared to a free machining material like brass. The machining forces in the cutting and thrust directions are recorded for a number of different chip thicknesses and rake angles, and the results for the two materials compared.

2. Static Tests (Free Machining Material). The variation of machining forces in the cutting and thrust directions with undeformed chip thickness is shown in Figure 5 for three different values of tool rake angle (α).

In all three cases, the machining forces show an approximately linear increase with undeformed chip thickness; except that, at a zero undeformed chip thickness, the cutting and thrust forces do not reduce to zero. These residual force components have been noted before by other investigators [9, 10, 17] and are now generally accepted as being the components of the tool nose force, which is assumed to be independent of undeformed chip thickness.

Comparison of the thrust force components in graphs (a), (b), and (c) of Figure 5 shows that the direction of the thrust force changes as the rake angle increases. At zero rake angle, it is positive and pushing the tool away from the workpiece and for a 20 deg rake angle, it is negative and pulling the tool into the workpiece. From these results, it is clear that the optimum rake angle for minimizing tolerance errors when machining brass is ten degrees.

By considering the intercept at zero chip thickness to be representative of the tool nose force and assuming that the tool nose force does not vary with chip thickness, then nose force can be plotted against rake angle to the first approximation. These results are shown in graph (d) of Figure 5 and suggest that the cutting component of nose force is larger than the thrust component for brass, and that the direction of the force turns toward the thrust direction as rake angle is increased.

3. Static Tests (Titanium). The variation of machining forces in the cutting and thrust directions with undeformed chip thickness when machining titanium is shown in Figure 6 for rake angles varying between 0 deg and 30 deg.

Comparing these results with those of Figure 5 shows that titanium exhibits the same cutting characteristics as a free machining material. The force variation with undeformed chip thickness is again a linear one, and again the direction of the thrust force changes from positive to negative as rake angle increases, but this time a rake angle of 20 deg would be the optimum for minimizing tolerance errors. The most noticeable difference between the two results is the higher intercepts in the case of the titanium, suggesting that the tool nose force for titanium is more significant.

The variation of nose force with rake angle, plotted from the intercepts of Figure 6, is shown in Figure 7. Again this result is only a first approximation and can be used only as a guide. It does suggest however for titanium that:

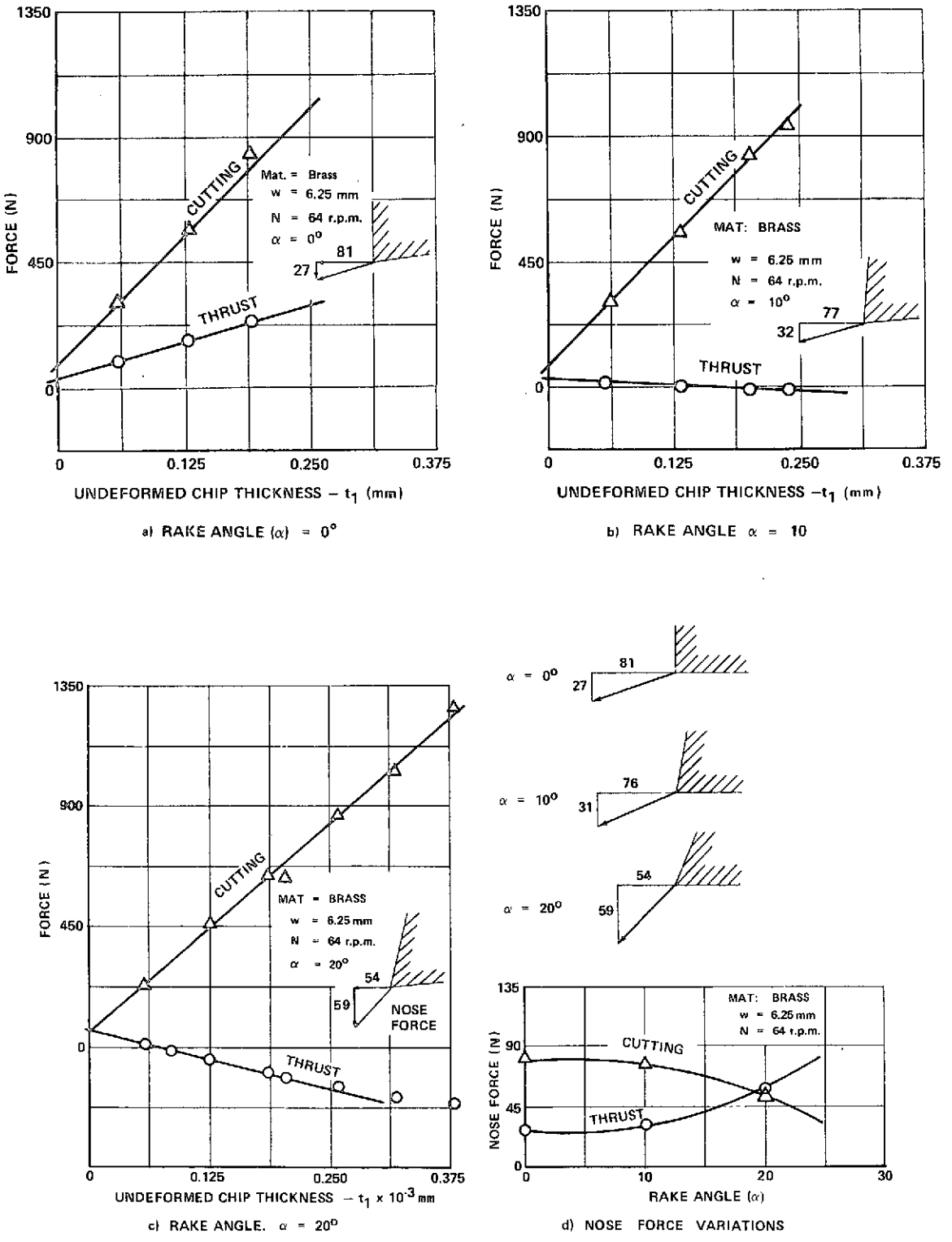

Figure 5. Variation of machining forces with undeformed chip thickness for different rake angles.

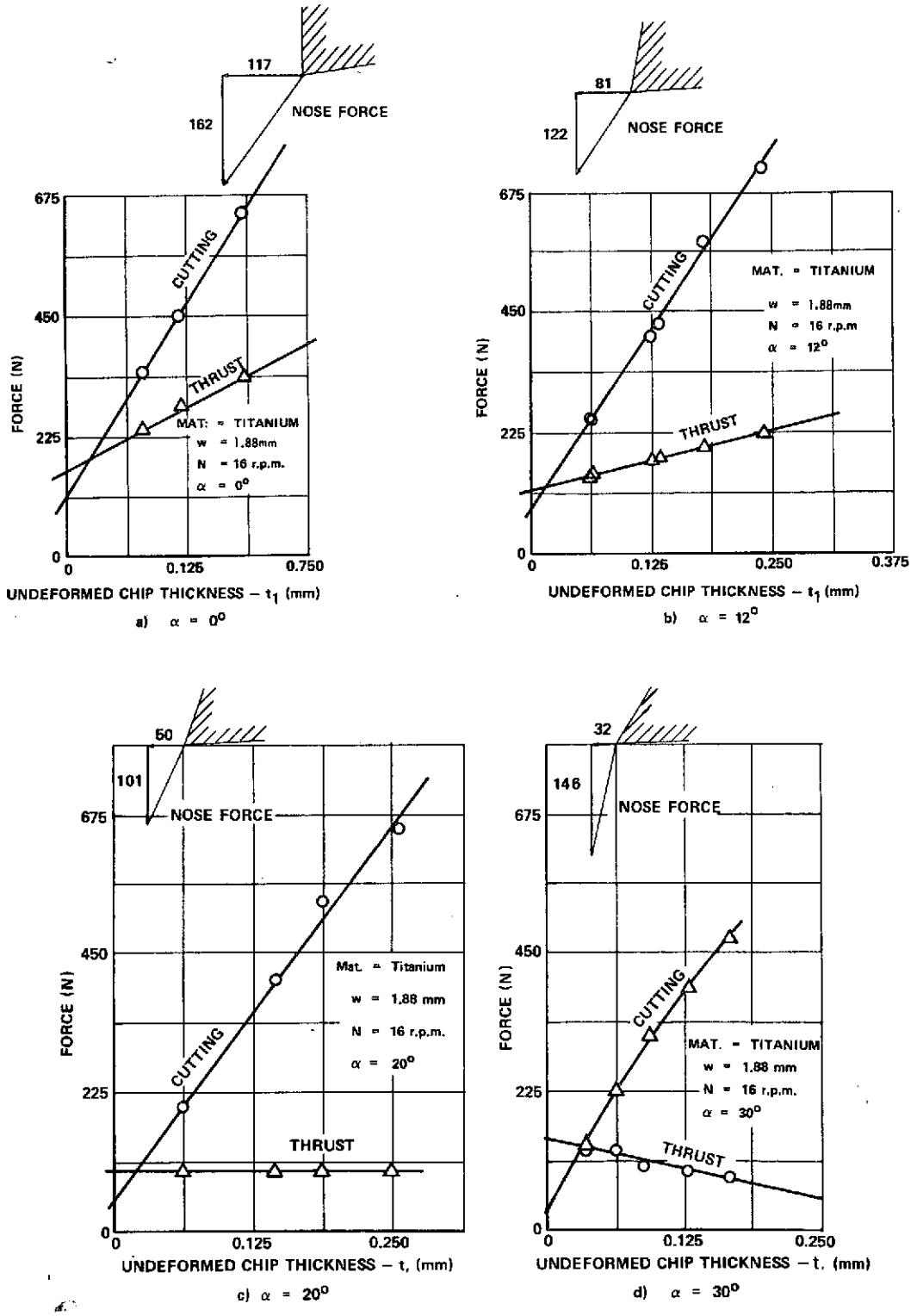

Figure 6. Variation of machining forces with undeformed chip thickness for different rake angles.

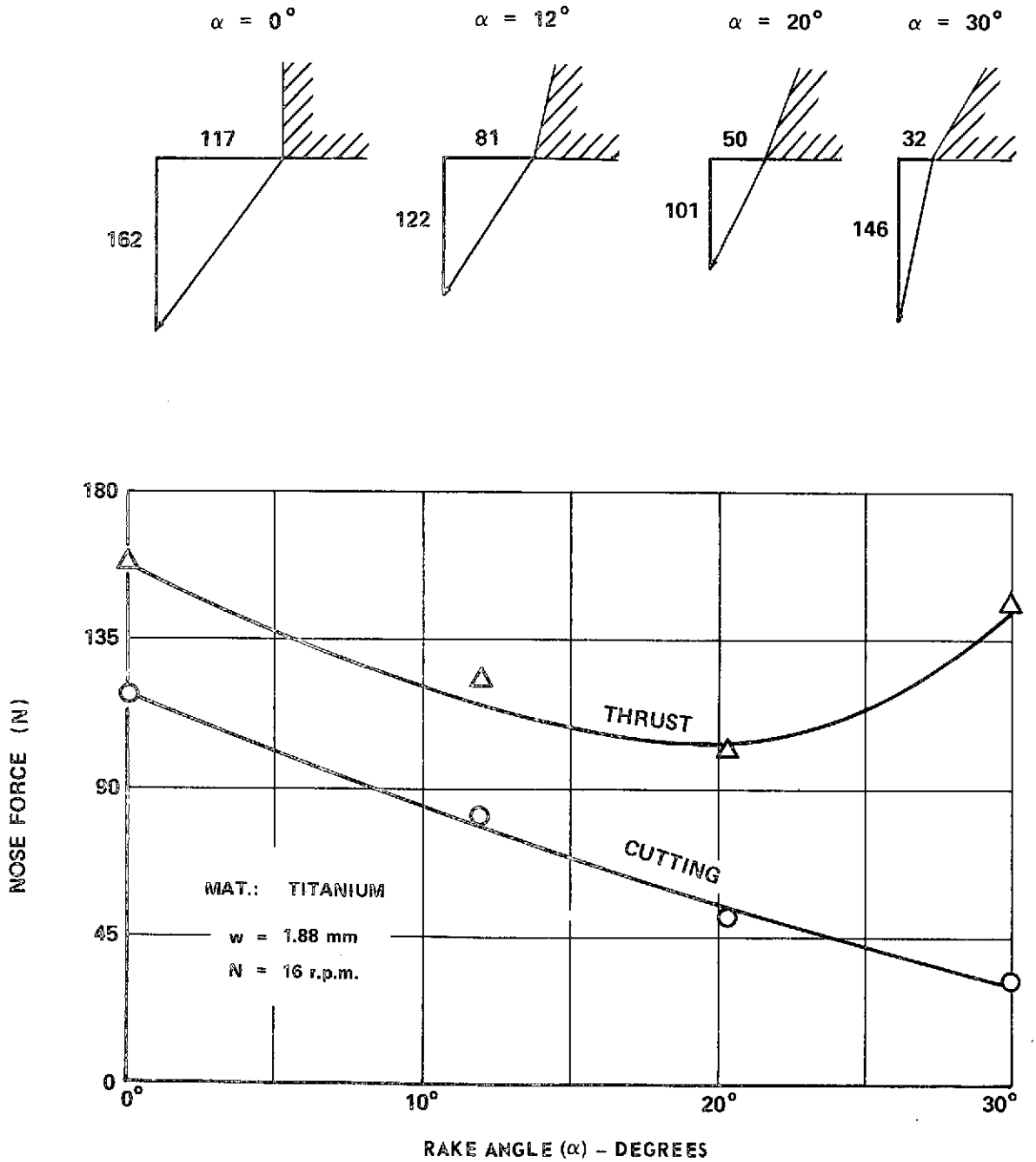

Figure 7. The variation of tool nose force with rake angle when machining titanium.

(1) Thrust component of the nose force is higher than the cutting component — the opposite was true for brass.

(2) The overall magnitude of the nose forces are larger. With the width-of-cut less, this implies that the nose force per unit length of cutting edge is much larger.

(3) The same rotation of the nose force toward the thrust direction is noticed as rake angle is increased.

4. Machining Titanium Compared to a Free-Machining Material. Table 1 gives a summary of the results presented so far and shows that the cutting pressure experienced when machining titanium are two and one-half times greater than those of brass for the same tool geometry. The tool nose force, however, can be as much as seven times larger, and the thrust component up to 20 times larger for titanium than for brass. This last result means that if the tool deflects only 0.005 mm (0.0002 in.) perpendicular to the cut surface when machining brass, it could deflect as much as 0.100 mm (0.004 in.) when machining titanium. Consequently, accurate finish machining of titanium could be a problem unless rigid fixtures are used.

TABLE 1. THE RATIOS OF STATIC CUTTING PRESSURE AND NOSE FORCE WHEN MACHINING TITANIUM, AS COMPARED TO BRASS

Rake angle (α) = degrees	Static cutting pressure (k_s)	Nose force/unit width (P_N)	Nose force in thrust dir^n/unit width (P_{N_t})
$\alpha = 0°$	2.6	7.8	20.0
$\alpha = 10°$	2.5	5.9	12.9
$\alpha = 20°$	2.6	4.7	6.3

The variation of the stress along the plane perpendicular to the shear plane is plotted against the length of the shear plane in Figure 8 for brass. The results show that the shear stress is constant and independent of chip thickness and rake angle, but that the normal stress or compressive stress is a function of rake angle (α).

The same results are plotted for titanium in Figure 9 and they show the same independence for shear stress, and rake angle dependence for normal stress, but also show that compared to brass, the normal or compressive stress is much higher.

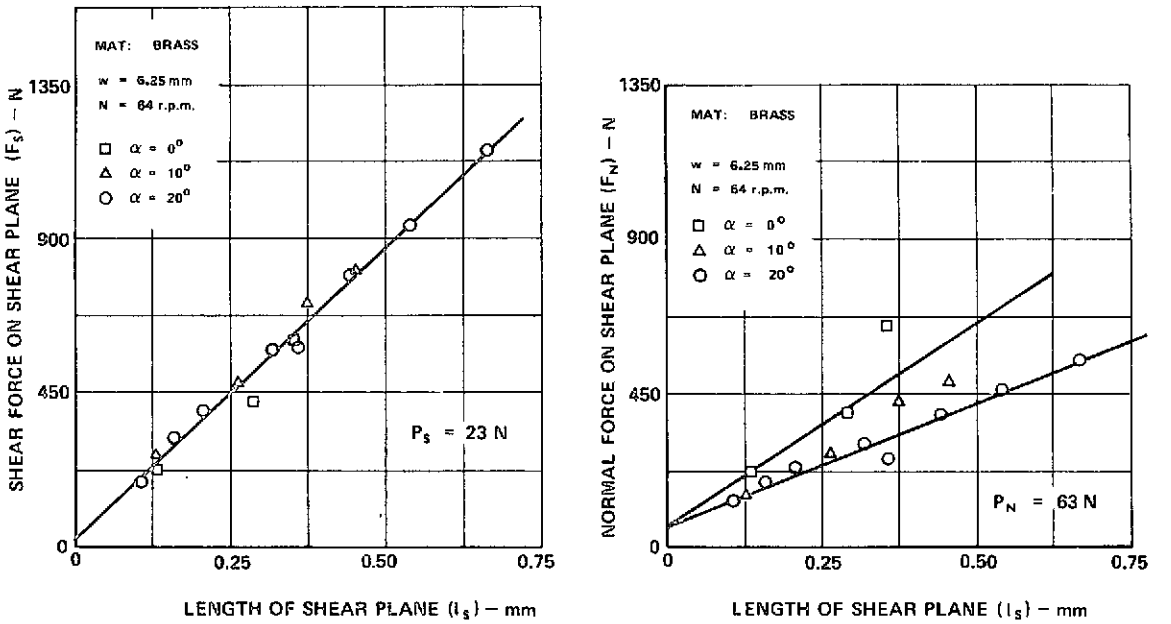

Figure 8. Variation of shear force and normal force with length of shear plane for brass.

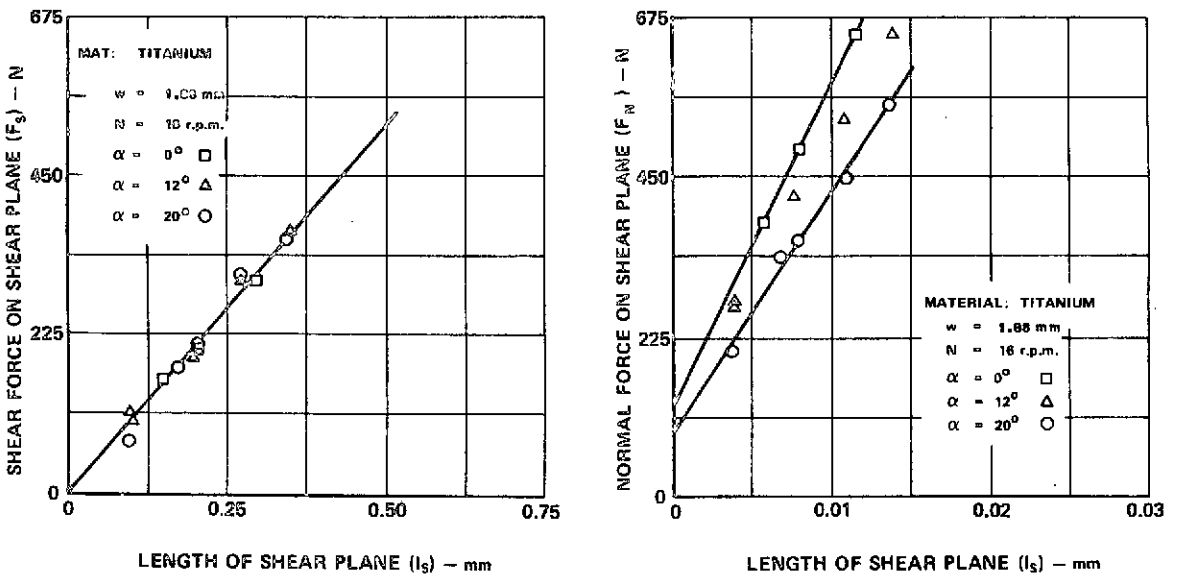

Figure 9. Variation of shear force and normal force with length of shear plane for titanium.

Table 2 is a summary of the shear plane results previously shown and shows that the ratio of shear stress for the two materials is only about two, whereas the ratio of compressive or normal stresses and nose forces for the same materials is about five or six times.

TABLE 2. MATERIAL PROPERTIES OF TITANIUM AND BRASS FROM MACHINING TESTS

Material	Shear Stress S_s - N/m^2	Normal Shear Stress S_N - N/m^2
Brass	2.63×10^8	$1.12 - 1.85 \times 10^8$
Titanium	5.16×10^8	$7.07 - 9.38 \times 10^8$
Ratio Titanium/Brass	1.92	5.07 - 6.31

This high compressive stress for titanium is probably due to its readiness to work harden and may explain the high nose forces also. The current theory is that some material passes under the flank of the tool and experiences compression and then elastic recovery [14,15]. If this is the case, then titanium's resistance to deformation, as indicated by its high shear angles (40 deg to 45 deg as opposed to 30 deg to 35 deg for brass) and high compressive stress, would cause high nose forces in the thrust direction, which was observed.

5. Material Properties. Static compression tests were performed on both titanium and brass, using a Tinius - Olsen 0 to 1,800,000 N (0 to 400,000 lbf) universal tester. The specimens measured 75-mm by 25-mm (3-in. by 1-in.) diameter and were machined from the materials that were used for the machining tests. Three specimens for each material were tested and the results for the 0.2 percent offset yield point were averaged. The results are compared in Table 3, with the normal or compressive stresses and the nose forces per unit width obtained from the machining tests described earlier.

It can be seen that the ratio of titanium to brass is of the same order for all the categories listed. These results, therefore, support the contention made in the previous section that the high nose forces associated with machining titanium arise from compression of the workpiece material under the flank of the tool. Moreover, the fact that the static compressive stress for the two materials is of the same order as the normal stress found from machining tests is a good indication that static compression tests can be used to determine whether a particular material is liable to produce high nose forces and poor machining tolerances.

TABLE 3. COMPARING THE MATERIAL PROPERTIES OBTAINED FROM MACHINING TESTS WITH THOSE FROM STATIC COMPRESSION TESTS

Material	Normal or Compressive Stress (N/m^2)	Nose Force Per Unit Width (N/m)	Static Compressive Stress‡ (N/m^2)
Brass	1.1 to 1.9×10^8	1.2 to 1.3×10^4	1.5×10^8
Titanium	7.1 to 9.4×10^8	5.9 to 10.0×10^4	9.6×10^8
Ratio of Titanium To Brass	5.1 to 6.3	4.7 to 7.8	6.3

‡ 0.2 percent offset yield

6. Discussion of Results. One major outcome of this investigation is that the tool nose forces when machining titanium are about seven times larger than the equivalent forces for brass. The cutting forces, however, are only about two and one-half time greater.

Any force in the thrust direction will have a detrimental effect on machining tolerances. The static cutting tests illustrate that the cutting forces in the thrust direction can be minimized for the two materials by choosing rake angles of 10 deg and 20 deg respectively for titanium and brass. The tool nose forces are determined by the amount of workpiece material compressed under the flank of the tool, and static compression tests show that the compressive stress for titanium is about six times higher than for brass, which suggests that this might be the reason the nose forces are higher for titanium. One way to minimize these forces is to reduce the amount of material compression under the tool by lapping a finer edge on it. This method of minimizing machining tolerances will be examined and discussed in a later section.

The static cutting tests have demonstrated how to minimize cutting force components in the thrust direction in order to reduce machining tolerances by optimizing the value of tool rake angle (α). The static compression tests demonstrate an easy method of evaluating whether a material will produce high nose forces when it is machined. The next section will examine the dynamic cutting characteristics of titanium compared to brass with particular emphasis of how the stability of the machining operation can be affected by machining speed and tool flank geometry.

F. Dynamic Cutting Tests

1. Previous Work. Vibration in machining has generally been investigated at conventional economic machining speeds, that is, speeds higher than are used for titanium. This is particularly true for work in turning and milling for which chatter and forced vibration cases have been examined in detail [18] at high speeds. The low speed condition in any machining operation is complicated by the machining forces losing their fixed phase relationship with the undeformed chip thickness variation. Smith and Tobias [19] in a brief survey quoted three workers who postulated lagging forces at low speeds, while they themselves found leading phase forces. Smith and Tobias, however, made no attempt to explain these discrepancies.

Results from a number of researchers have been correlated [13] to indicate the general trends of vibration problem at low speeds for a number of different machining processes. The chief outcome of this survey was that all the machining operations examined exhibited a stabilization at lower speeds, attributed by the author to be caused by contact between tool flank and machined surface. Sisson and Kegg [5], in an extension of the previous work, showed that the same effect existed when turning titanium — in fact they suggested that low speed stability was independent of workpiece material.

A more detailed analysis of the cutting forces was performed by Wallace and Andrew [12]. Their work was restricted to simple orthogonal turning operations. They examined wave-cutting (i.e., removing an initially flat surface with a vibrating tool) and showed qualitative and quantitative evidence of a leading phase oscillatory thrust force (penetration force) proportional to the rate of change of tool vibration amplitude — i.e., directly proportional to the change in clearance angle. They also showed that the amplitude of this thrust force increased with flank length, but did not examine the quantitative effects of this.

Sisson and Kegg [5], in examining low speed stability, first noticed that decreasing the clearance angle increased stabilization, and postulated that other factors might also affect stability in this way.

The above review of previous work indicates that the variables affecting low speed stability are not entirely established.

It is proposed to test the theory presented in equations (18) and (19) and to measure the amount of damping by plotting the dynamic cutting pressure in the thrust direction (R_t/wX), and its phase relative to tool motion (θ_t),

against the inverse of wavelength ($1/\lambda$) for a range of clearance angles (γ_m). The justification of this approach has been discussed earlier in the Stability Analysis Section.

It is also proposed to examine other variables, such as flank land (1), to see how they affect these quantities and so stability.

2. Dynamic Tests (Free Machining Material). The variation of the dynamic cutting pressure in the thrust direction is plotted against $1/\lambda$ in Figure 10(a). It can be seen that the amplitude of the dynamic cutting pressure increased as the wavelength (λ) gets smaller, and that the smaller the clearance angle (γ_m) becomes, the larger this increase is. When the same results are plotted against ($1/\gamma_m\lambda$) in Figure 10(b), it can be seen that all the points fall on one single curve. This suggests that the dynamic cutting pressure is inversely proportional to both wavelength (λ) and clearance angle (γ_m). The theoretical curve is from equation (18) with values of k_q and k_t chosen by curve fitting. The solid points occur when the wavelength is small enough for cutter flank/workpiece interference to take place. This criterion is a function of both vibration amplitude and wavelength and is given in equation (22).

Figure 11 shows how the phase of the dynamic cutting pressure relative to the chip thickness variation varies with $1/\lambda$ and $1/\gamma_m\lambda$. Again, there is the same dependence on clearance angle (γ_m), such that the results in Figure 11(b) fall on a single curve.

It can be seen that as wavelength decreases, the dynamic cutting pressure in the thrust direction leads the undeformed chip thickness variation by a phase angle approaching 90 degrees and so has a stabilizing influence. When the wavelength is reduced to a value where tool/workpiece contact occurs, equation (20), it can be seen that this phase lead of the dynamic cutting pressure tends towards 45 degrees. Examination of a typical recording for this condition (Figure 12) shows that as the tool moves into the workpiece contact occurs and the force variation may be non-linear due to the occurrence of an additional contact force for only part of the vibration cycle. This non-linearity causes fluctuations in the phase (θ_t), between the dynamic cutting pressure in the thrust direction and tool motion, that make phase measurement both difficult and meaningless.

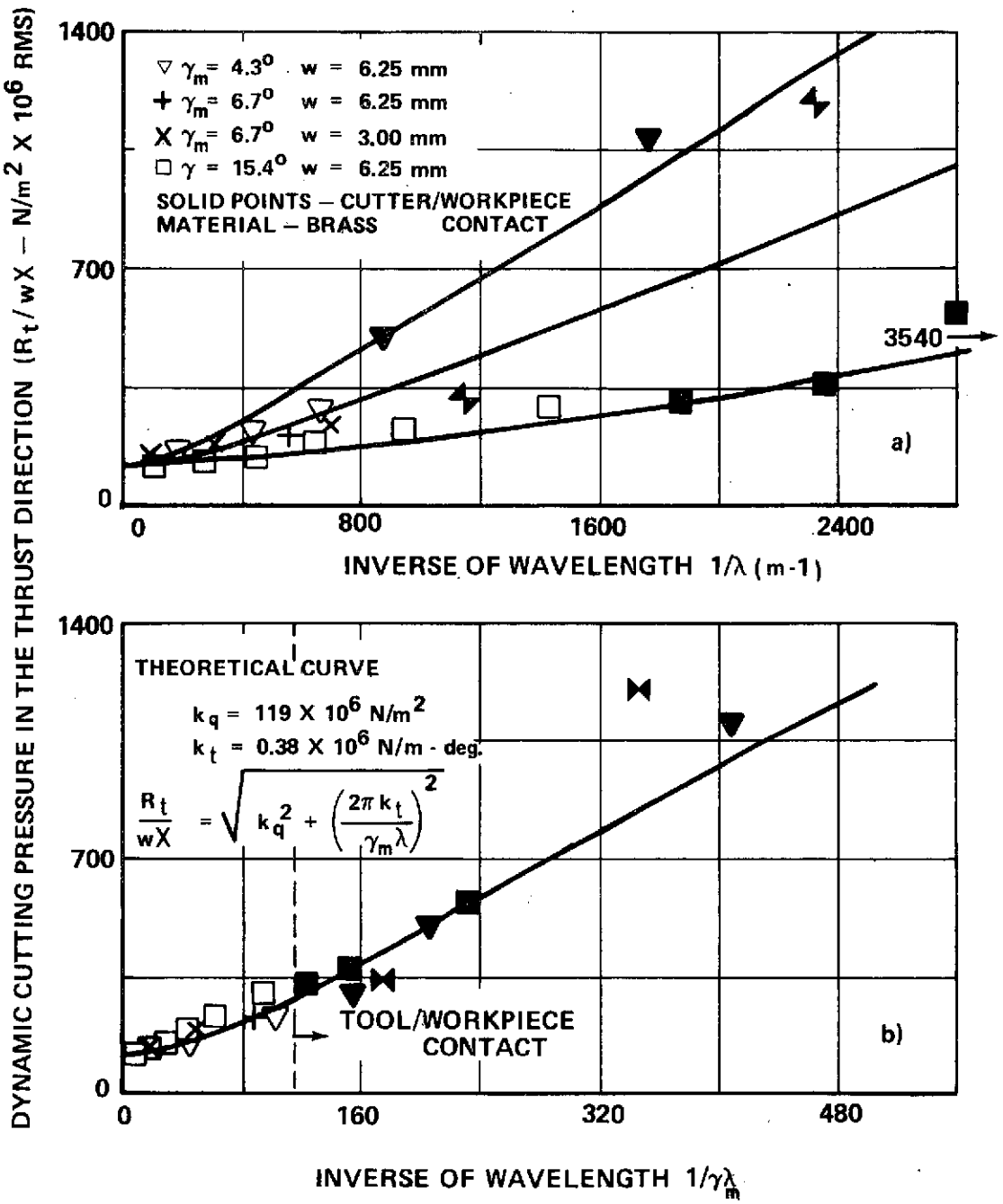

Figure 10. The effect of clearance angle (γ_m) on the cutting pressure in the thrust direction – Brass.

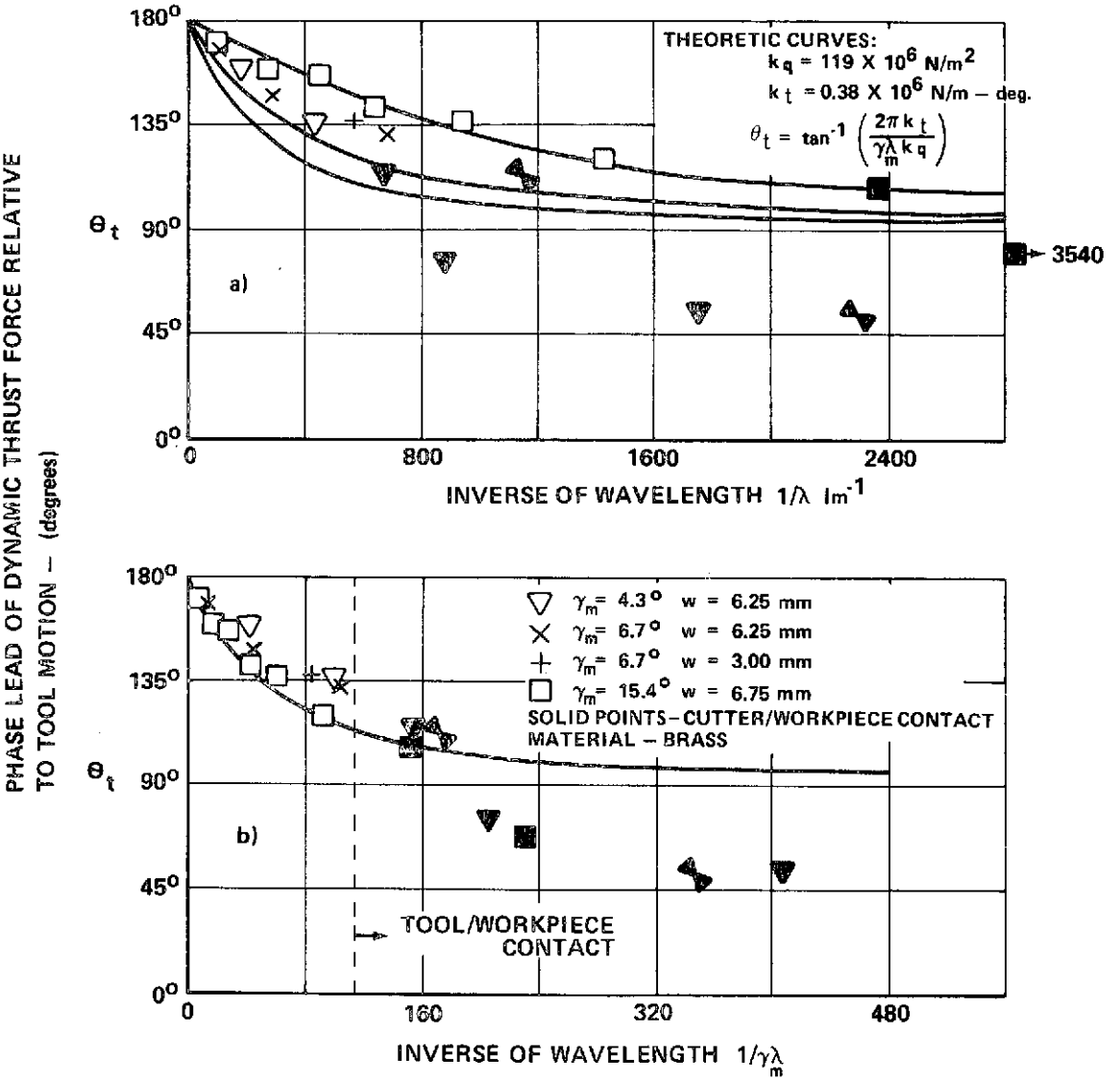

Figure 11. The effect of clearance angle on the phase lead of dynamic Tl thrust force relative to tool motion — brass.

The effect of a change in rake angle (α) on the dynamic cutting pressure in the thrust direction and its phase relative to tool motion (θ_t) is shown in Figure 13. There is no noticeable difference between these two sets of results and it can be concluded that a variation in rake angle has little effect on the dynamic cutting pressure characteristics.

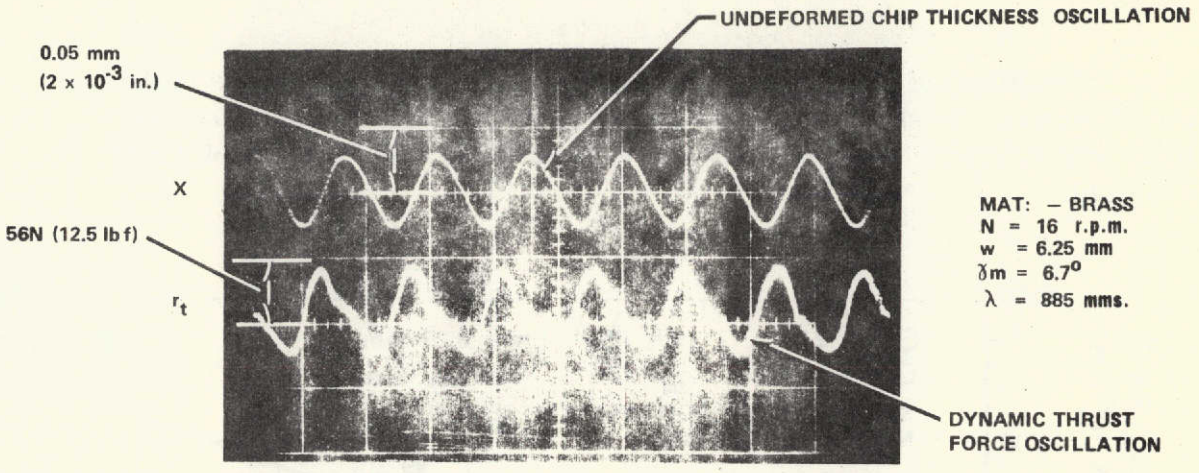

a) TYPICAL TRACE OF THE DYNAMIC THRUST FORCE SHOWING NON-LINEAR DUE TO THE CONTACT FORCE (p_c)

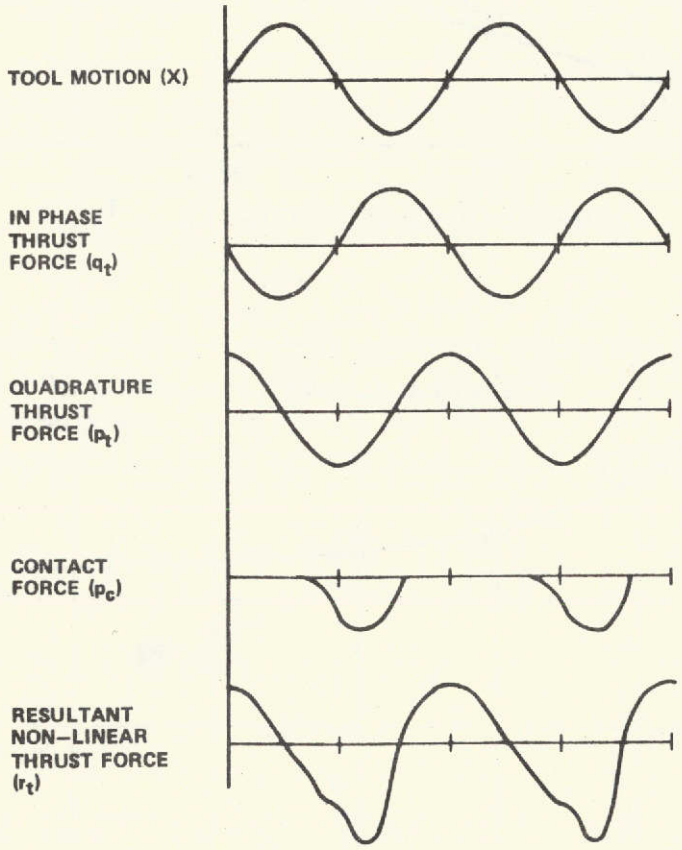

b) SCHEMATIC REPRESENTATION OF HOW THE CONTACT FORCE ARISES.

Figure 12. The contact force showing:
a) typical trace of the dynamic thrust force
b) schematic representation of how the contact force arises.

The effect of a flank land (1) on the dynamic cutting pressure in the thrust direction is shown in Figure 14 where results using a sharp tool and tools with 0.125mm (5×10^{-3} in.) and 0.250mm (10×10^{-3} in.) flank lands are used.

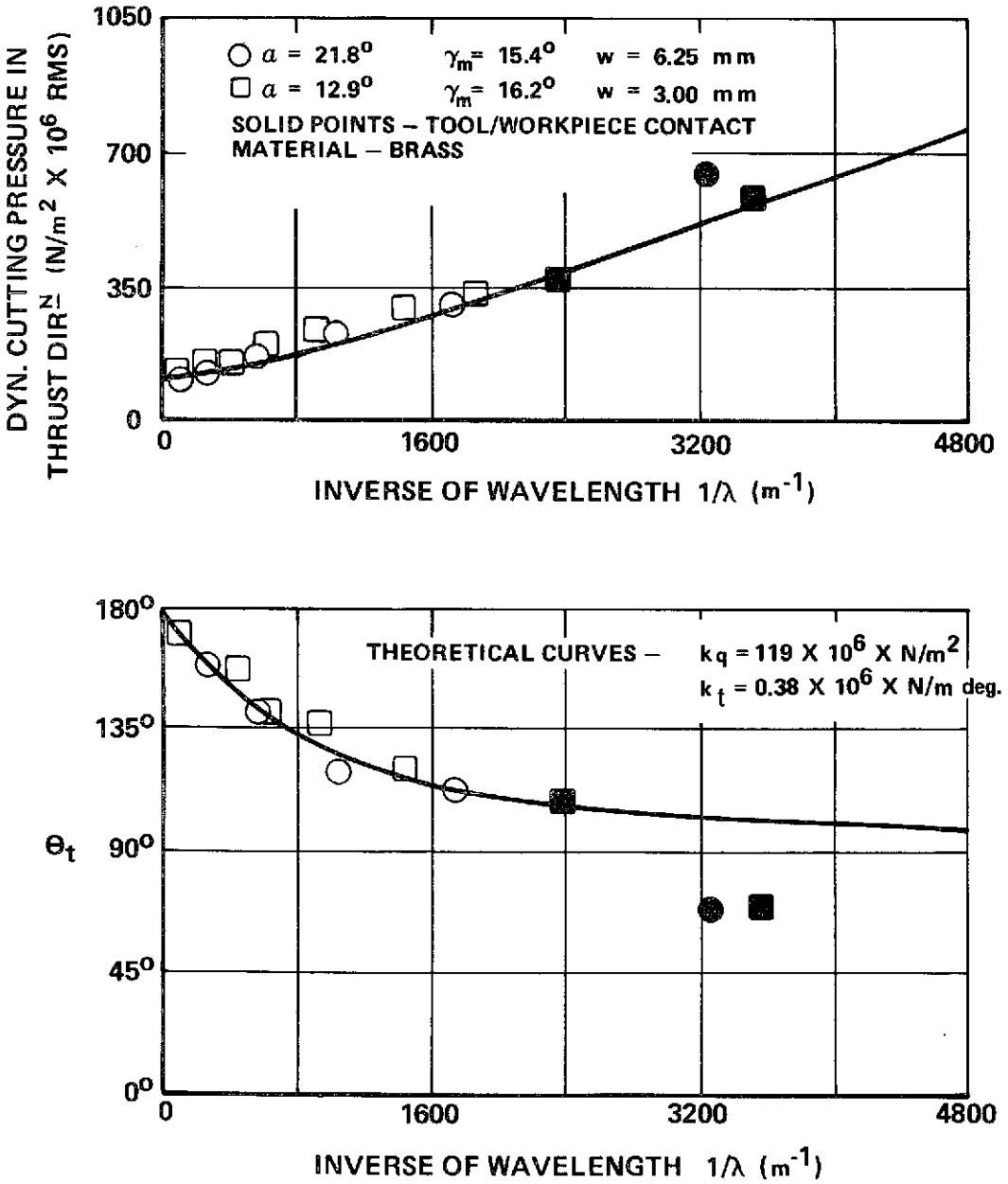

Figure 13. The effect of rake angle (α) on cutting pressure and θ_t.

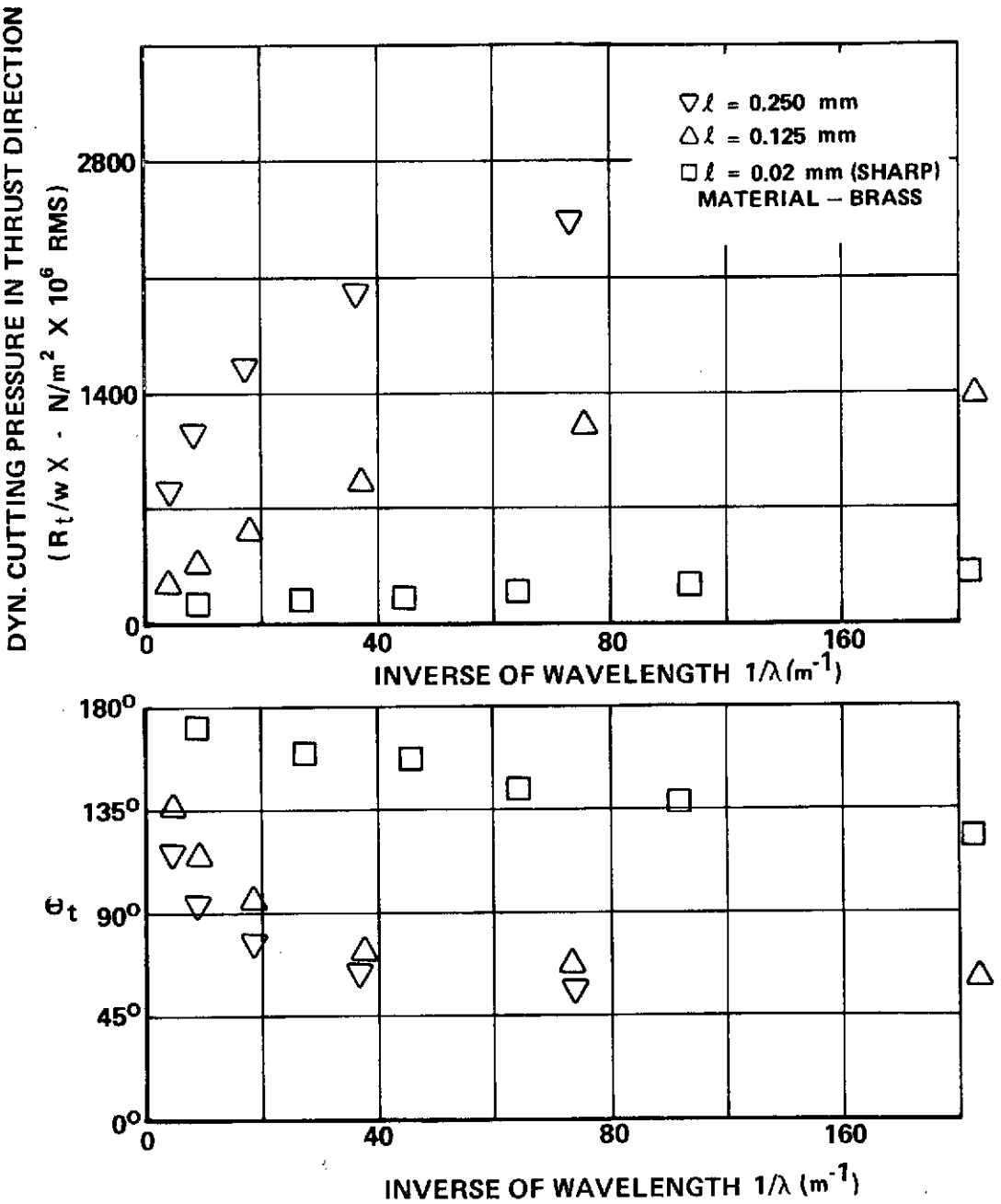

Figure 14. The effect of flank land (l) on dynamic cutting pressure in the thrust direction — brass.

The resuls show that adding a flank land increases the dynamic cutting pressure considerably — the larger the land, the larger the increase. The phase between the dynamic cutting pressure and tool motion (θ_t) can be seen to approach 90 deg at a much larger wavelength than for a sharp tool. This suggests that if a stabilization force were required at higher machining speeds, where the wavelength of vibration are larger, then it could be obtained by grinding a flank land on the tool.

The results of Figure 14 are plotted in Figure 15 against l^2/λ and show that the dynamic cutting pressure in the thrust direction is a function of the flank land (l) as well as its size relative to the wavelength (l/λ). This dependence on l^2/λ can be written into the theoretical variation of equation (18) to give the empirical curve shown with the results in Figure 15. The experimental results agree well with this theoretical curve up to a cutting pressure of about 700×10^6 N/m^2 (1.0×10^5 lbf/in.^{2}). Above this point, measured cutting pressures are lower than expected, which is probably due to the cutting pressure causing yield in the material.

3. Dynamic Tests (Titanium). The variation dynamic cutting pressure in the thrust direction with $1/\lambda$ and $1/\gamma_m\lambda$ is shown in Figure 16, graphs (a) and (b), respectively, for two different values of clearance angle (γ_m). The results show the same dependence on clearance angle for titanium as for brass, but with a more noticeable increase in cutting pressure due to tool/workpiece contact.

The phase of the dynamic cutting pressure in the thrust direction relative to tool motion (θ_t) is plotted against $1/\gamma_m\lambda$ and shown in Figure 17. Because the in-phase cutting force acts in a direction which is almost parallel to the direction of cutting, the component of in-phase dynamic cutting pressure is in the thrust direction and hence (k_q) is small, so that the phase of the overall dynamic cutting pressure relative to tool motion (θ_t) approaches 90 deg even for large wavelengths. However, as the amplitude of this pressure is low at these wavelengths, phase differences become difficult to measure, which is why the theoretical curve is drawn towards both in-phase and out-of-phase conditions (i.e. the dynamic cutting pressure could be in-phase or out-of-phase with tool motion depending upon the dynamic cutting force acting on one side or the other of the cutting direction). The phase relationship (θ_t), after tool/workpiece contact has occurred, tends towards an in-phase condition where stabilizing qualities are lost.

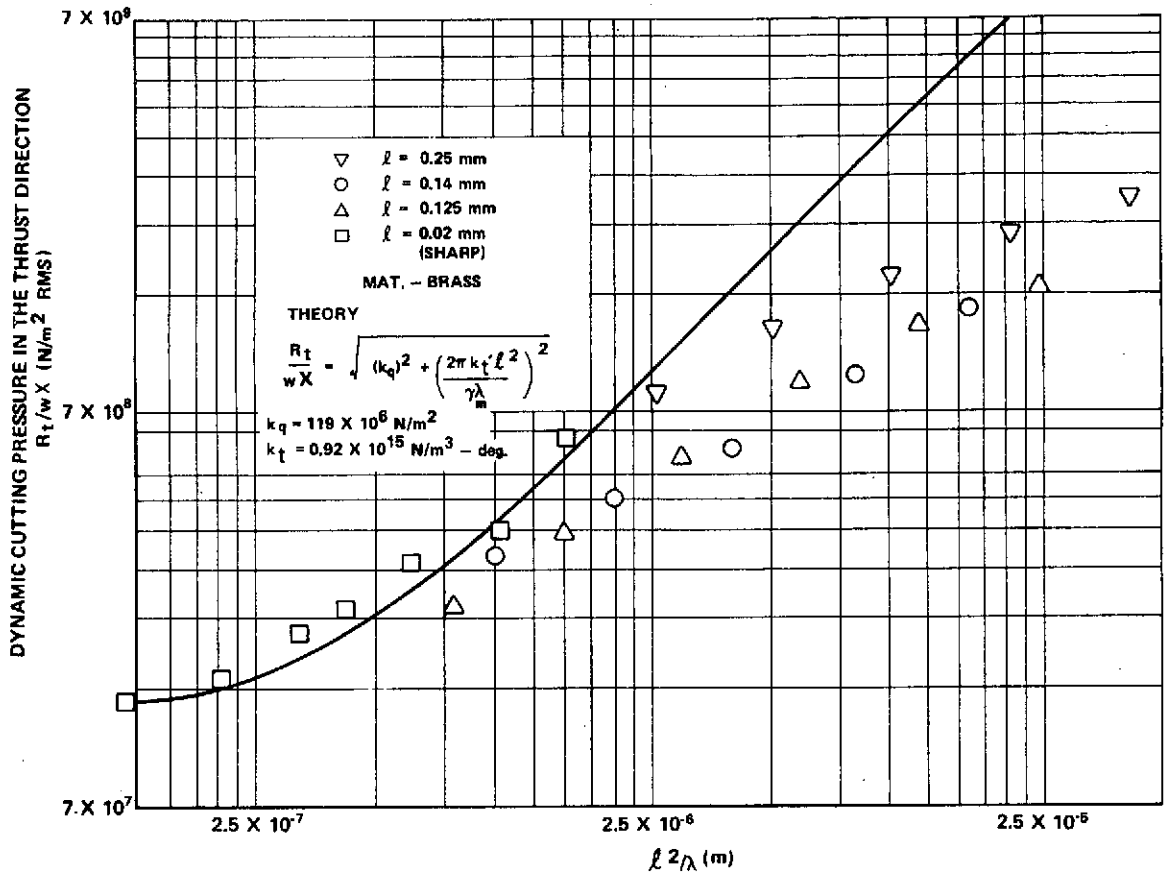

Figure 15. The variation of dynamic cutting pressure in the thrust direction with l^2/λ for different flank lands (l) and wavelengths (λ) — brass.

The variation of dynamic cutting pressure with l/λ for various rake angles is plotted in Figure 18. It can be seen that the points fall on a single curve at low values of wavelength (λ), but at the intercept where $l/\lambda = 0$, the value of k_q is different for different rake angles. This is to be expected, since a change in rake angle will produce a change in the direction of orientation of the in-phase cutting pressure, and will consequently modify the resolved in-phase component of dynamic cutting pressure in the thrust direction. However, the value of k_t is the same as was used throughout the titanium tests, so that it can be concluded that the penetration in the thrust direction is independent of rake angle.

The variation of dynamic cutting pressure in the thrust direction with l/λ is shown in Figure 19 and demonstrates that introducing a flank land increases these thrust pressures considerably. Plotting the same results against l^2/λ in Figure 20 shows that titanium behaves in a similar way to brass, but suggests a higher compressive yield stress for the material.

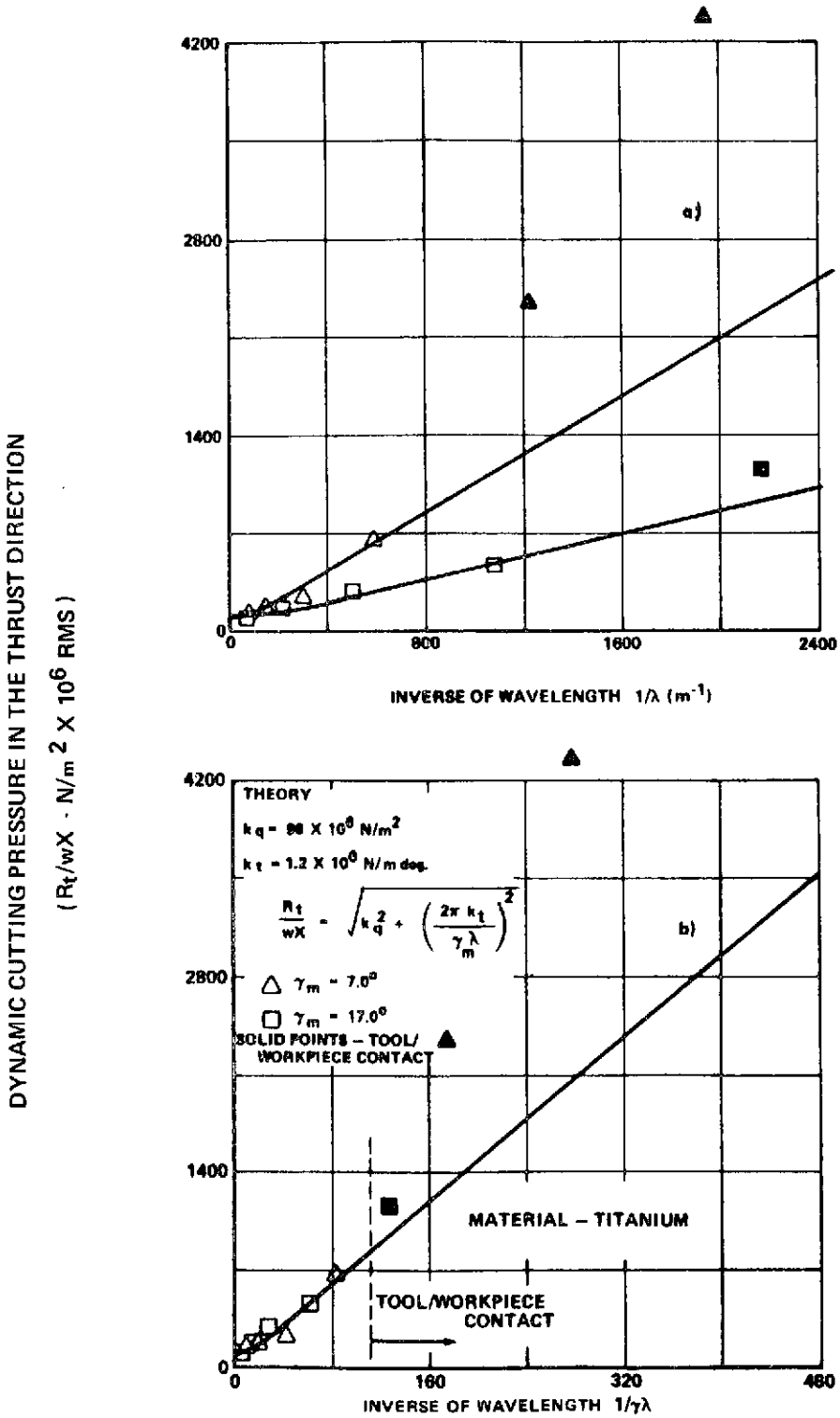

Figure 16. The effect of clearance angle (γm) on the cutting pressure in the thrust direction – titanium.

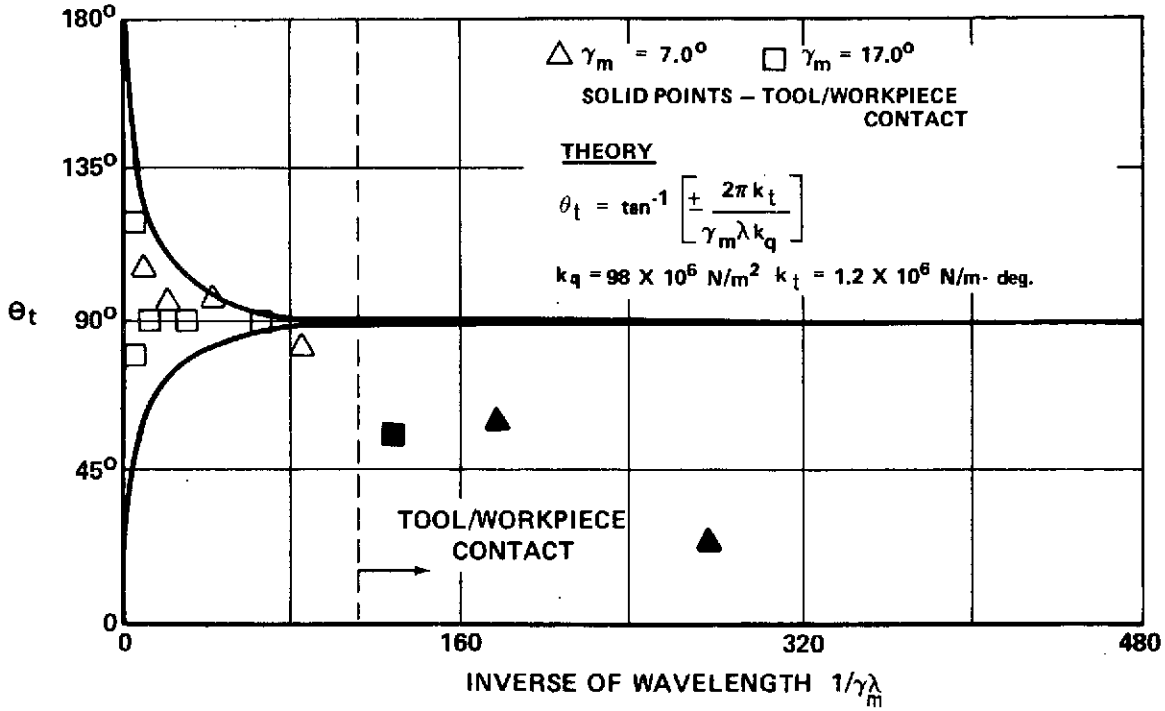

Figure 17. The variation of θ_t with $1/\gamma_m\lambda$ — titanium.

4. Discussion of Results. The results show that the dynamic cutting pressure in the thrust direction due to flank contact is a quadrature stabilizing force and that it is a function of the metal cutting process. The workpiece material is only found to affect the magnitude of this stabilizing force.

The results of these tests substantiate the predictions of equation (24), that the penetration coefficient (K*) is inversely proportional to wavelength (λ) and clearance angle (γ_m) and in addition shows that this coefficient is proportional to the second power of flank land (l^2) and independent of rake angle (α).

They also show that the rake angle can affect the in-phase component of cutting pressure in the thrust direction (k_q), which substantiates that k_q is a function of $\sin(\tau-\alpha)$.

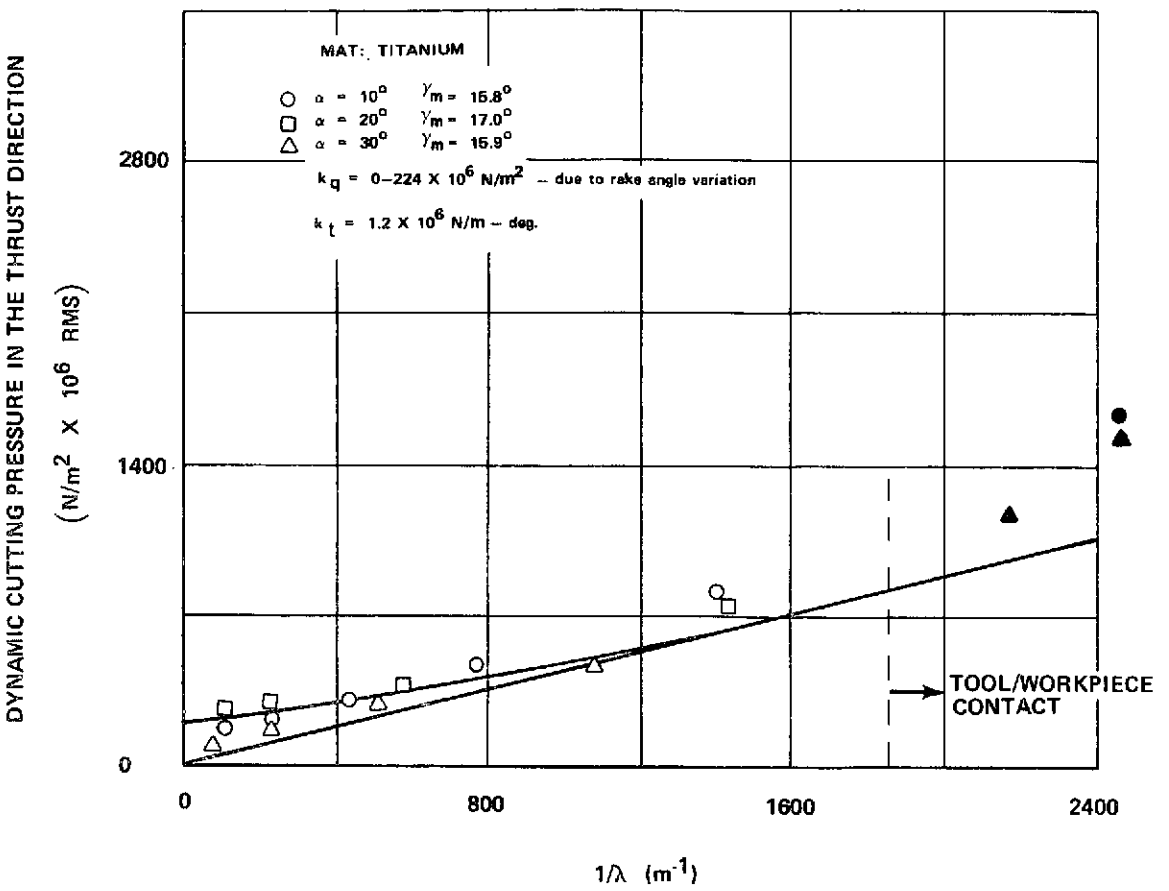

Figure 18. The effect of rake angle (α) on the dynamic cutting pressure in the thrust direction — titanium.

The results also show that the penetration coefficient (k_t) is three times as large for titanium as for brass, indicating a higher stabilization potential for titanium, provided (k_q) is kept small by the choice of rake angle (α).

It has already been established by Tobias [15], that increasing width of cut (w) can lead to instability for any material. Because the speed of machining titanium is limited by high tool tip temperatures which causes tool breakdown, it is necessary to machine titanium at a speed where productivity is low and machining costs are high. If machining feeds and widths can be increased to offset this reduction in machining speed, then hopefully machining costs can be reduced.

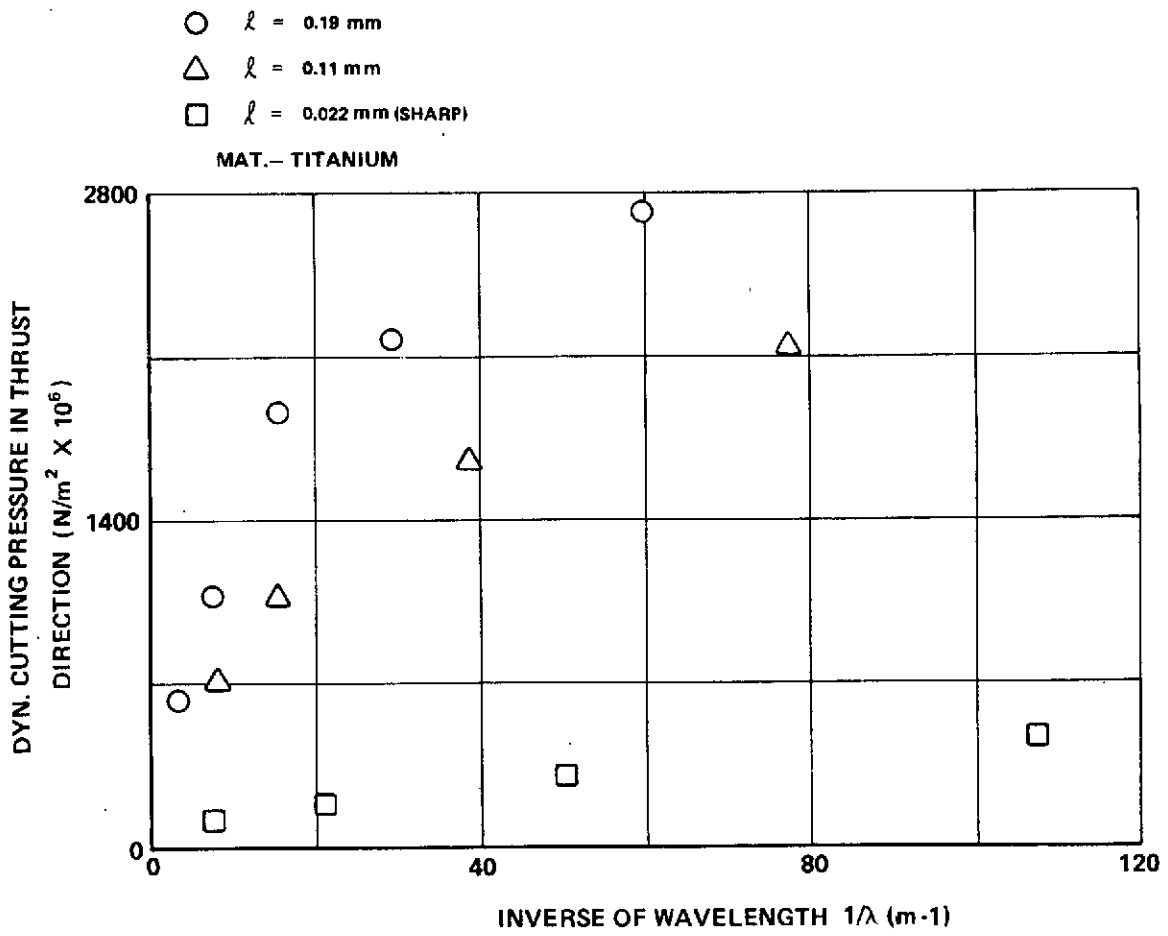

Figure 19. Effect of flank land (l) on dynamic cutting pressure in thrust direction – titanium.

The main limitation to increasing the feed is increasing the tool tip temperature and hence tool wear – this will be examined in a later section.

Increasing the width of cut however spreads the load on the tool tip and so does not affect the machining temperature directly. Instead, it increases the cutting forces to a level where instability can easily occur.

The results of this section therefore give a number of options:

(i) If a machinist has to lower his cutting speed to machine a material like titanium, then the process will become inherently more stable, meaning that he can increase his width of cut.

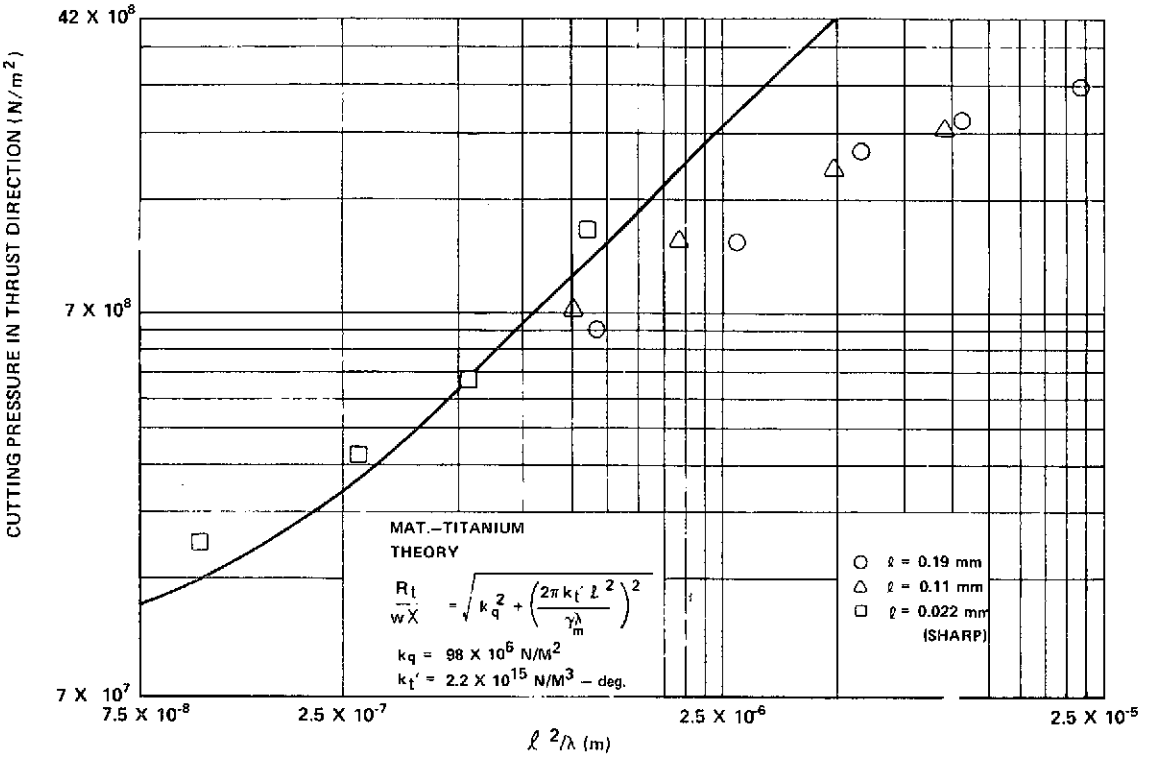

Figure 20. The variation of dynamic cutting pressure in the thrust direction with l^2/λ for different flank land (l) and wavelengths (λ) — titanium.

(ii) He can maximize stability by minimizing clearance angle.

(iii) If he encounters a bad case of chatter, and he has tried the above procedures without success, he can still grind a land on the flank of the tool to increase stability. However, this is only recommended as a desperation procedure, since it reduces the life of the tool and may increase tool tip temperatures.

Although all of these recommendations add damping to a vibrating system, it should be remembered [15] that a stiff machine tool is a prerequisite for machining difficult-to-machine materials without chatter.

G. The Effect of New Tool Materials and Surface Treatments on the Machining of Titanium

Review. The high cutting temperatures, when machining titanium, are associated with the unusually high shear angles and hence high chip velocities, together with a small contact area between chip and tool. This, coupled with the lower thermal conductivity and low specific heat of titanium, gives rise to unusually high tool tip temperature [4].

One possible solution to the problem is either to find an additional tool ingredient that would extend its useful life or to protect the tool with a thin, temperature resistant layer.

Wicher and Pope [20] have found that the titanium carbide (TiC) content of a tungsten carbide (WC) tool increases the tool's thermal conductivity and allows increased cutting speeds for a given tool life. In machining steels and cast irons, Stanislao, et al [21], also found that adding TiC to tungsten carbide tooling increased thermal conductivity but attributed the reduced tool wear to reduced tool tip temperature caused by the formation of a protective film of Ti203 during machining.

Ljungquist [22] describes the recent development of TiC cemented carbide inserts, that utilize Chemical Vapor Deposition (CVD) to deposit a hard, but brittle, TiC layer of high wear resistance on a tough core of tungsten carbide (WC). He finds that thicker layers lead to a longer tool life provided the coating stays on.

Mayer and Cowell [23] describe a cemented titanium carbide tool, developed at Ford Motor Company, that surpasses the life expectancy of a TiC coated tungsten carbide tool. Figure 21 shows an example of one of Mayer's tool life curves where he compares a conventional tungsten carbide (WC) tool with a TiC coated tungsten carbide tool and a cemented TiC tool. It can be seen that the TiC coated tool wears at the same rate as the cemented TiC tool until its coating is worn through, whereupon, it resumes the wear rate of the conventional tungsten carbide (WC) tool.

All the above investigators, however, have been machining high strength steels. Unfortunately, when cemented TiC or coated TiC tungsten carbide tools are used to machine titanium or any of its alloys, the oxygen in the $Ti_2 0_3$ lubricating film reacts with the titanium in the workpiece and reduces the lubricating properties of the film [22].

Suh [24] has shown that oxide treatment of tungsten carbide tools can increase tool life by up to 80 percent. So far he has had success using titanium dioxide, zirconium oxide, aluminum oxide, chromium sesquioxide, and tantalum oxide. However, his tool life tests were restricted to AISI 4340 steel and his results may not apply when machining titanium. In fact, Shaw and Nakayana [4] suggest that both Ceramic and Oxide tools form particularly strong bonds to titanium and exhibit poor life compared to tungsten carbide.

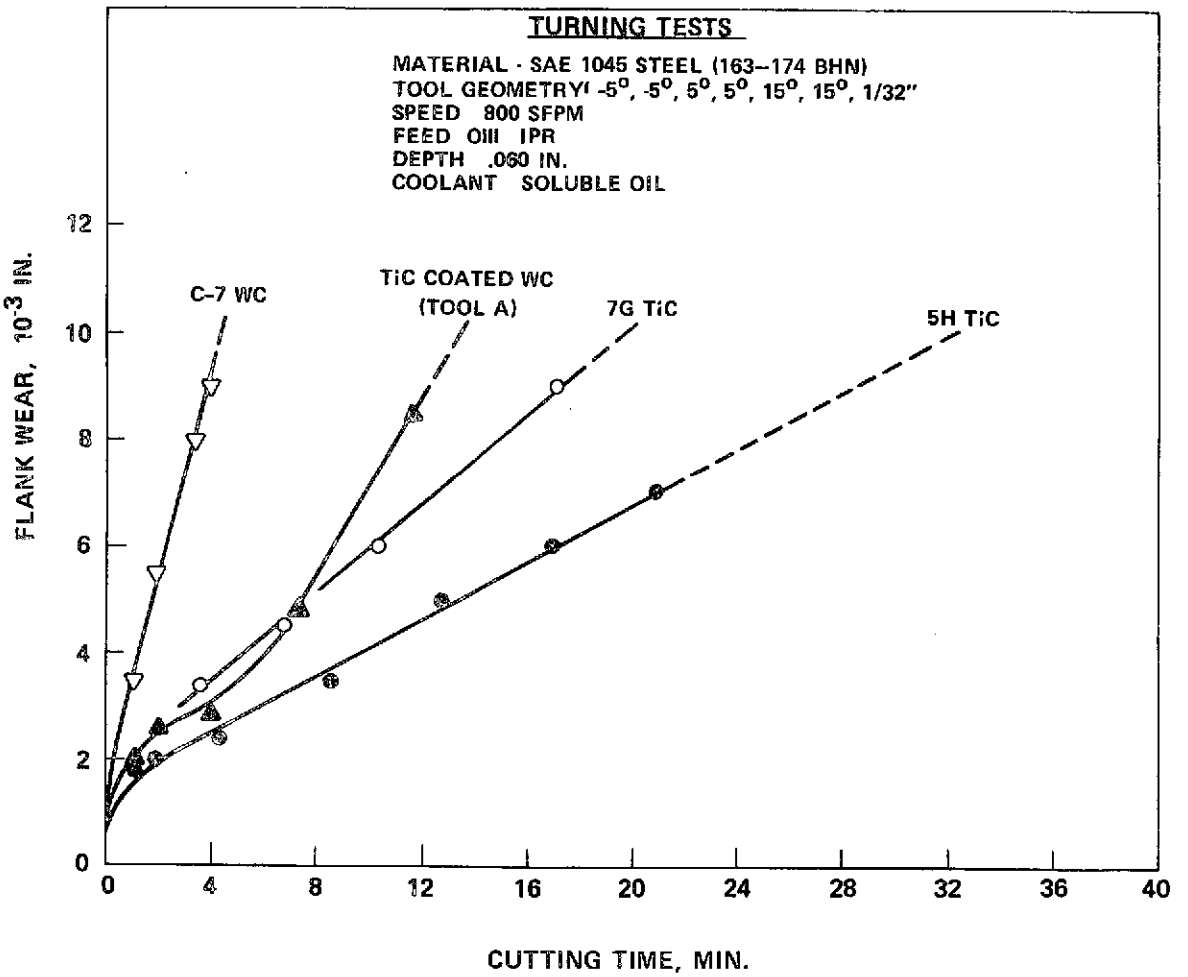

Figure 21. Flank wear comparison of 5h and 7g titanium carbide grades and c-7 tungsten carbide grade against titanium carbide coated cemented tungsten carbide tool A [23].

Titanium, therefore, is difficult to machine due to the lack of a suitable tool material to machine it with. Hopefully, a tool coating or material can be developed that will produce a suitable lubricating film that will protect the tungsten carbide core and yet will not react with the titanium being machined. Although the author accepts the need for further research in this area, it is not the intention of this investigation to get involved with developing new materials.

The simple conclusion is that a general purpose carbide is the best known tool material for machining titanium and in the next section we will examine ways of getting maximum usage out of it.

H. The Effect of Tool Finish on Machining Tolerance and Tool Life

1. Introduction. The lack of tool reliability has been a source of concern for production planners for a long time. For otherwise identical machining conditions, tool life can vary significantly from one tool to another. This suggests that there are variables affecting tool life that are not understood. Kane and Zimmers [25] examined the influence of surface roughness and grinding direction on tool life for carbide and HSS tools. The surface roughness ranges they examined were from "precision ground", 0.1 to 0.15 micrometers (4 to 6 microinches), to "as sintered", 0.75 to 1.00 micrometers (30 to 40 microinches). They found that the sintered tool wore out at about twice the rate of a precision ground tool, and that the direction of the grinding marks on a tool can influence its life up to about 25 percent.

They found that tool life was decreased most where the direction of grinding was perpendicular to the cutting edge on both the flank and the rake forces of the tool and that optimum wear conditions were obtained when the direction of grinding was parallel to the cutting edge on the flank face and perpendicular to the edge on the rake face of the tool, with parallel grinding to the cutting edge on both surfaces running a close second.

The effects of different grinding techniques on tool life have been examined by Montag and Lierath [26]. They compared electrolytic grinding and diamond wheel grinding, with a 100-grit wheel; with conventional grinding, using a SiC wheel. They found that electrolytic grinding gave a longer tool life compared to SiC, particularly when the wheel was allowed to spark out either mechanically or electrically. Grinding with a diamond wheel improved tool life, when compared to SiC, but not to the extent found using electrolytic grinding.

They found that letting the wheel spark-out with a zero feed condition inproved the tool surface and cutting edge finish and they concluded that this along with the "cool grind" obtained with electrolytics was one major reason why tool life was extended.

From the above review it was decided to examine the effect of improved tool surface finish on tool life when machining titanium. As Montag and Lierath obtained a significant tool life improvement using a 100-grit diamond wheel, it was decided to use a 1800-grit diamond lap so that grinding temperatures could be kept as low as possible and surface finishes of less than 1 microinch could be achieved.

2. Tool Grinding and Machining Test Procedures. The method of grinding the tools in a conventional manner has already been described in the Test Procedure section. The lapped tools are just "touched" on a 1800-grit diamond impregnated grinding wheel mounted on a Leonard Grind-r-lap. The grinding wheel used was a new design [27] that gave a finish of less than one microinch (RMS) with negligible tool heating.

The machining force tests were performed in the same manner as the static tests described earlier. The tool wear tests were run on a Monarch, Model 61 lathe with a 13 inch chuck machining titanium (Ti-6A1-4V) from the same stock as previous tests. The tools used were a general purpose, C-2 tungsten carbide ground with the following tool angles:

Side rake	=	10 deg
Back rake	=	10 deg
End relief	=	3 deg
End clearance	=	8 deg
Side relief	=	3 deg
Side clearance	=	8 deg
Side cutting edge	=	10 deg
End cutting edge	=	18 deg
Nose radius	=	0.25mm

Each tool was mounted in line with the centerline of the workpiece and machined to give an undeformed chip width of 1.25mm (0.050 in.).

The wear land on the flank of the tool was measured approximately every 15 minutes so that a wear rate could be established. The tool life was considered for convenience to be reached when the flank land approached 0.125mm (5×10^{-3} in.). This was chosen in preference to 0.25mm or 0.5mm in order to conserve workpiece material. The wear lands were measured to within $\pm$ 0.0025mm, using a toolmakers' microscope.

A typical flank wear land versus time result is shown in Figure 22. It can be seen that after an initial high rate of wear, the wear rate stabilizes and becomes constant. The arbitrary tool life measured at a flank land of 0.125mm (5×10^{-3} in.), 15 hours or 900 minutes in the case of Figure 22, may be ambigous considering that a tool could be used until a wear land of 0.5mm or 1.0mm was reached or workpiece surface finish deterioration started. Unless the tool actually breaks down, tool life is difficult to measure. In this study, therefore, the stabilized wear rate is recorded as well as the overall wear rate that includes the initial accelerated tool wear. These slopes are drawn in Figure 22, and it can be seen that they envelope the result and give an estimate of maximum and minimum wear rate, from which the respective minimum and maximum tool life for a flank wear land of 0.125mm (5×10^{-3} in.) can be calculated. The tool life tests were run without coolant to examine:

(i) The effect of feed at a constant speed of 27 surface meters per minute (90 surface feet per minute).

(ii) The effect of speed at a constant feed of 0.0128 mm/rev. (0.0051 inches/rev.).

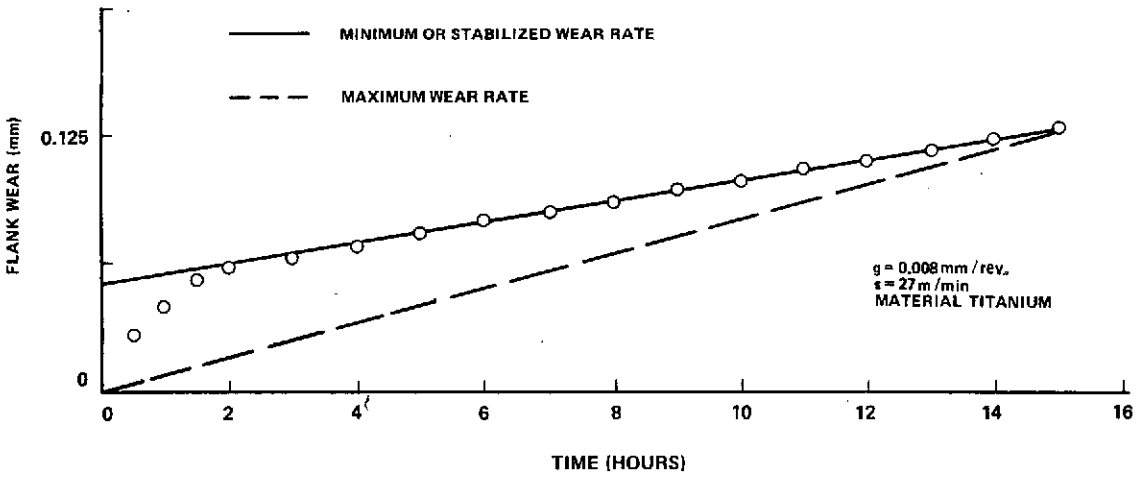

Figure 22. A typical tool flank wear with time curve.

These tests were first performed using the conventionally ground tools and then repeated using the lapped tools. Tools were reground after each tool life test using the same grinding procedure.

3. Results of Machining Force Tests. The variation of machining force in the cutting and thrust directions with undeformed chip thickness is plotted in Figure 23, graphs (a), (b), and (c) for three different rake angles.

The results, when compared with Figure 6, graphs (a), (b), and (c), which were identical machining conditions but with a conventionally ground tool, show that although there is no significant difference in the slope of the curves (i.e., the specific cutting pressure), there is a significant reduction in the tool nose force components obtained from the intercept at zero chip thickness.

The results for the conventionally ground tool shown in Figure 6(b) are plotted with those of the lapped tool shown in Figure 23(b) and reveal that for large undeformed chip thicknesses, there is no difference between the two tools. However, when chip thickness is reduced and the nose force becomes significant compared to the cutting force, then the lapped tool shows a marked improvement.

The variation of tool nose force, obtained from the intercepts in the previous results, is plotted against rake angle (α) in Figure 23(d). It can be seen that the thrust component of nose force is still larger than the cutting component, but that it is reduced for all values of rake angle compared to the results for a conventionally ground tool.

Table 4 shows that the nose forces for a lapped tool are about a factor of two and one-half times larger for titanium than for brass, which is more in line with the difference in cutting pressure of the two materials shown in Table 1.

The variation of machining force in the cutting and thrust directions with undeformed chip thickness for a TiC coated, lapped carbide tool, is shown in Figure 24. When this result is compared with Figure 23(a), it can be seen that the introduction of a TiC layer on the tool does not significantly alter the cutting coefficient. Its only effect is to increase the nose force, probably due to the TiC layer increasing the nose radius of the tool.

The nose forces for a conventionally ground tool, a lapped tool and a TiC coated tool are compared in Table 5 for a constant rake angle of zero degrees.

4. Results of Tool Life Tests. The effect of feed and speed on stock removal, which is the product of feed, speed, width-of-cut and tool life, is shown in Figure 25 graphs (a) and (b), respectively. The shaded areas represent the minimum values and the unshaded areas the maximum values of

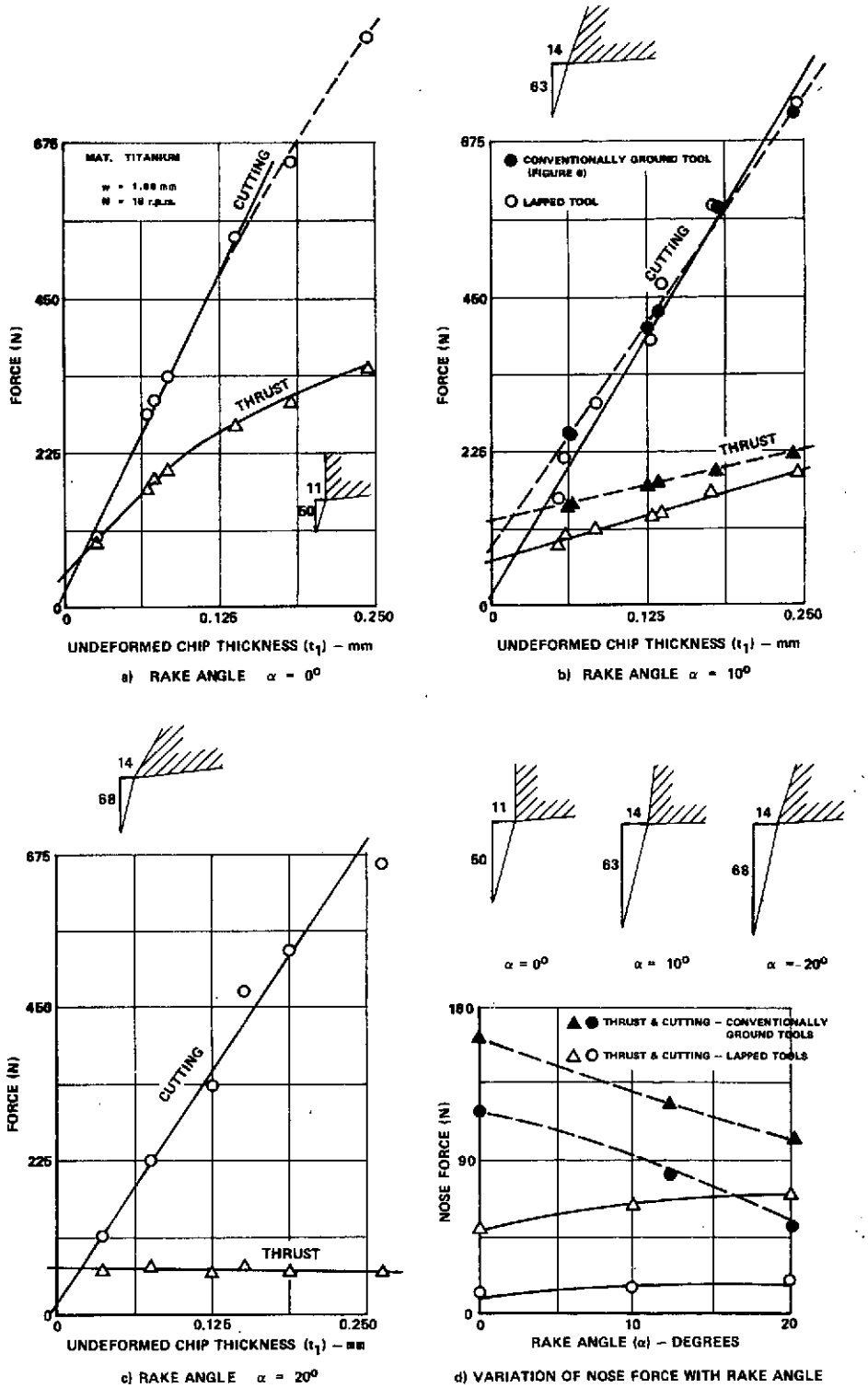

Figure 23. The variation of machining forces with undeformed chip thickness for different rake angles — using a lapped tool.

TABLE 4. THE EFFECT ON NOSE FORCE OF LAPPING THE TOOL

Rake Angle (α)	Nose Force/Unit Width*	
	Conventionally Ground	Lapped
0°	7.8	2.0
10°	5.9	2.6
20°	4.7	2.9

*All ratios are based on nose forces machining brass with a conventional ground tool.

stock removal corresponding to the different extremes of tool life obtained from the extrapolation techniques described earlier and illustrated in Figure 22. It can be seen that for maximum stock removal during the life of the tool, that a feed of about 0.19mm/rev. (0.0075 in./rev.) and a speed of about 42m/min. (140 ft./Min.) should be used. The same result is observed when using a lapped tool (Fig. 26), except that more stock removal is possible during the life of the tool. It was found that the reduced stock removal at high speeds and feeds was due to a sudden drop in tool life, while the drop in stock removal at low speeds and feeds was a function of both tool life decreasing and the speeds and feeds themselves decreasing.

The drop in tool life at low metal removal rates, compared to the sharp drop off at high metal removal rates, is shown to be small in Figure 27, where tool life is plotted against the rate of stock removal, which is a product of speeds, feed, and width-of-cut. Each result represents the average of four tests. The mean tool life in Figure 27 is 33 percent higher and the optimum rate of stock removal is 7 percent higher for the lapped tool than for the conventionally ground tool.

The variation of stock removal with the rate of stock removal is shown in Figure 28. The result is essentially the same as the previous results, except that plotting the stock removal during the life of the tool against the rate of stock removal is a more valuable result in terms of manufacturing economics. There is now a much more distinct optimum, and the results show that the mean stock removal is 42 percent higher and the optimum rate of stock removal is again 7 percent higher for the lapped tool than for the conventionally ground tool.

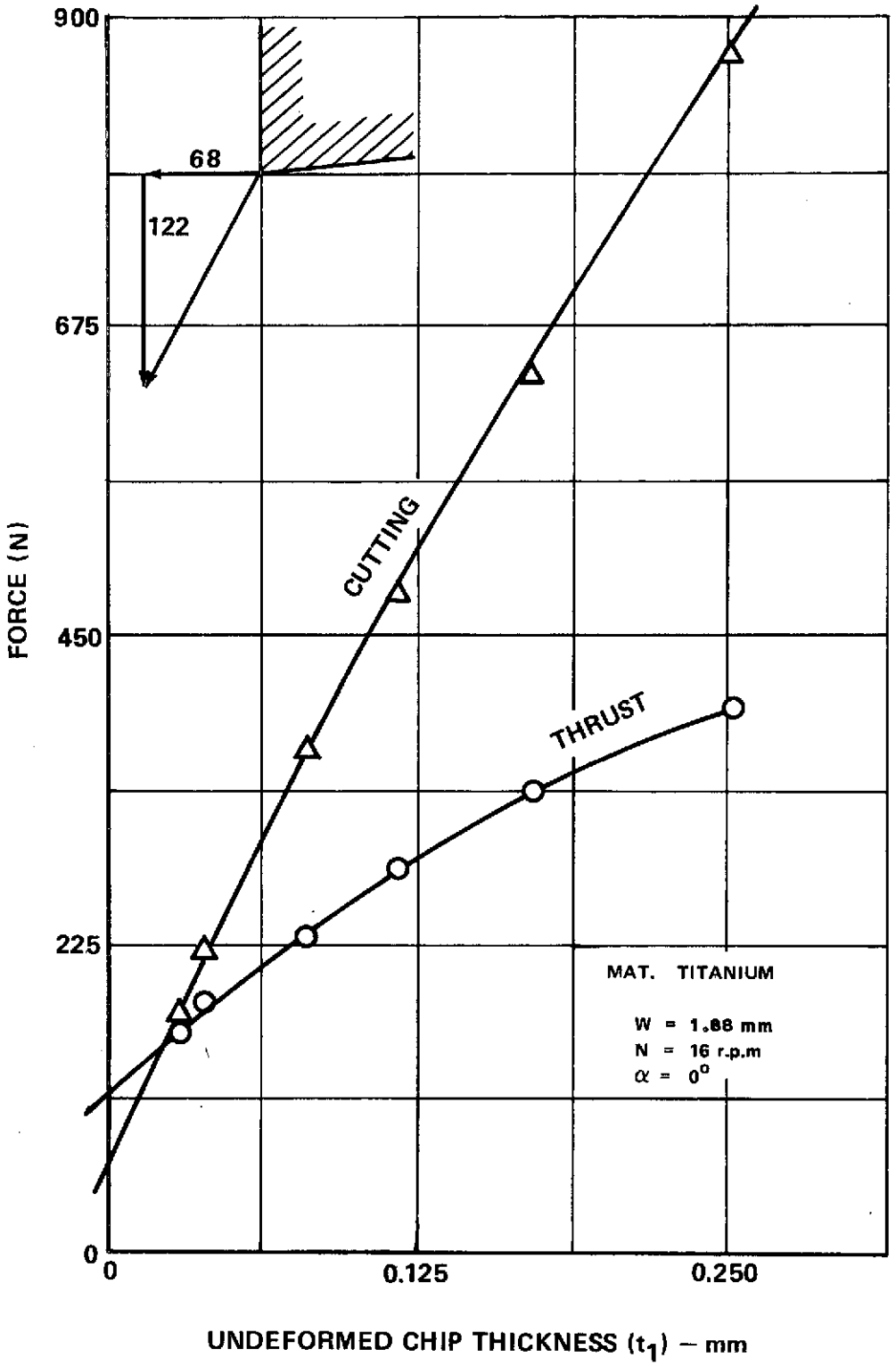

Figure 24. The variation of machining forces with chip thickness for a TiC coated tungsten carbide tool.

TABLE 5. TOOL NOSE FORCES FOR A TiC COATED TOOL COMPARED TO CONVENTIONALLY GROUND OR LAPPED TOOLS

	Machining Brass	Machining Titanium		
	Conventionally Ground Tool		Lapped Tool	TiC Coated Tool
Thrust Force (N)	27	162	50	122
Cutting Force (N)	81	117	11	68
Total Nose Force (N)	86	198	51	140
Nose Force Per Unit Width (N/m)	1.35×10^4	10.5×10^4	2.7×10^4	7.2×10^4
Compared to Brass	1	7.8	2.0	5.3

Machining Conditions

Brass	Titanium
N = 64 r.p.m.	N = 16 r.p.m.
w = 6.25 mm	w = 1.88 mm
t_1 = 0.125 mm/rev.	t_1 = 0.125 mm/rev.
α = 0°	α = 0°

5. Discussion of Results. Lapping a tool after grinding it has two effects when machining titanium:

(1) The nose force is reduced by about 50 percent.

(2) Tool Life is increased by about 30 percent.

The high thrust nose forces obtained when machining titanium, and their influence on machining tolerances, have been discussed earlier. Lapping the tool is one method of reducing these forces and consequently machining to closer tolerances.

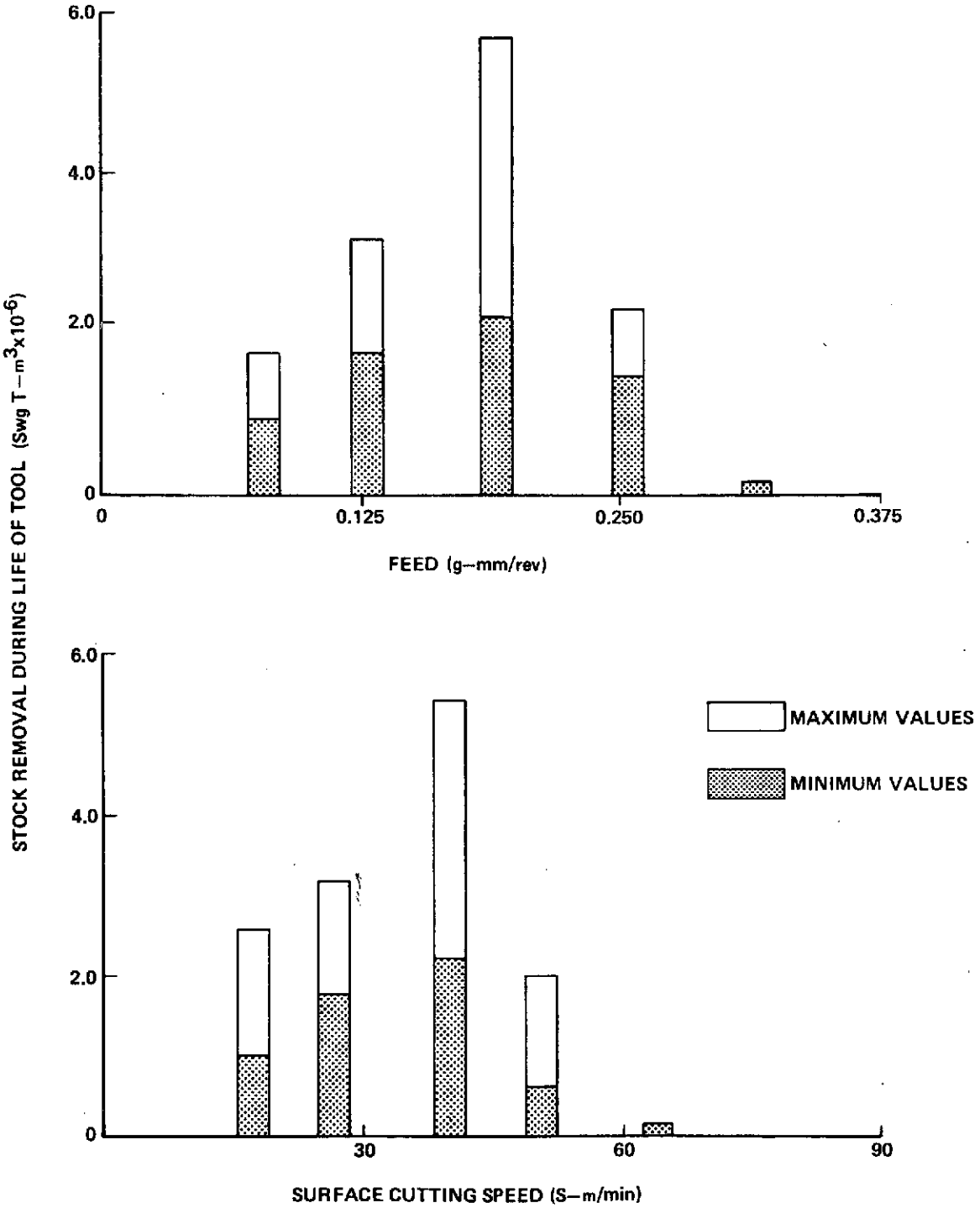

Figure 25. The effect of a) feed and b) speed on the stock removed during the life of a conventionally ground tool.

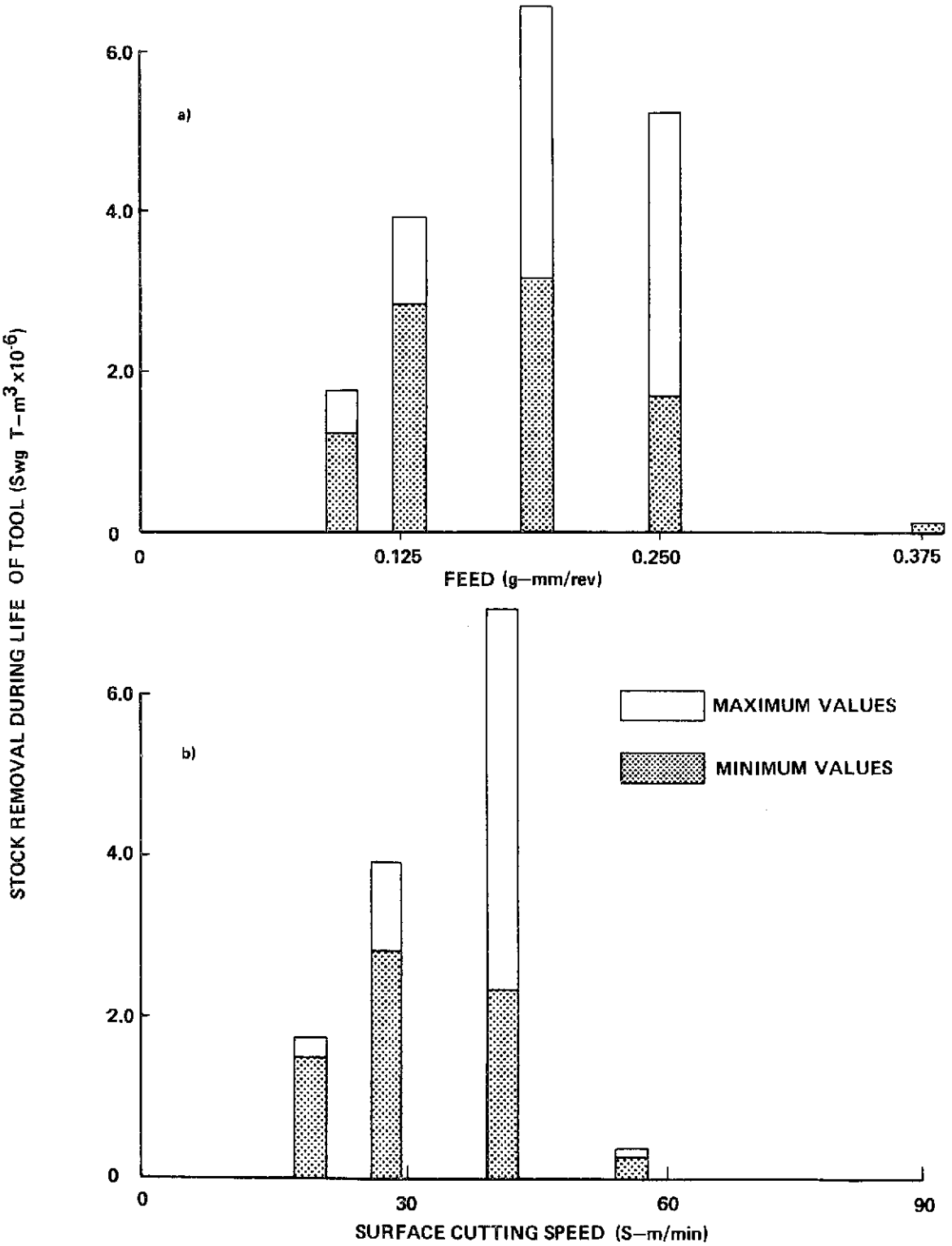

Figure 26. The effect of a) feed b) speed on the stock removed during the life of a lapped tool.

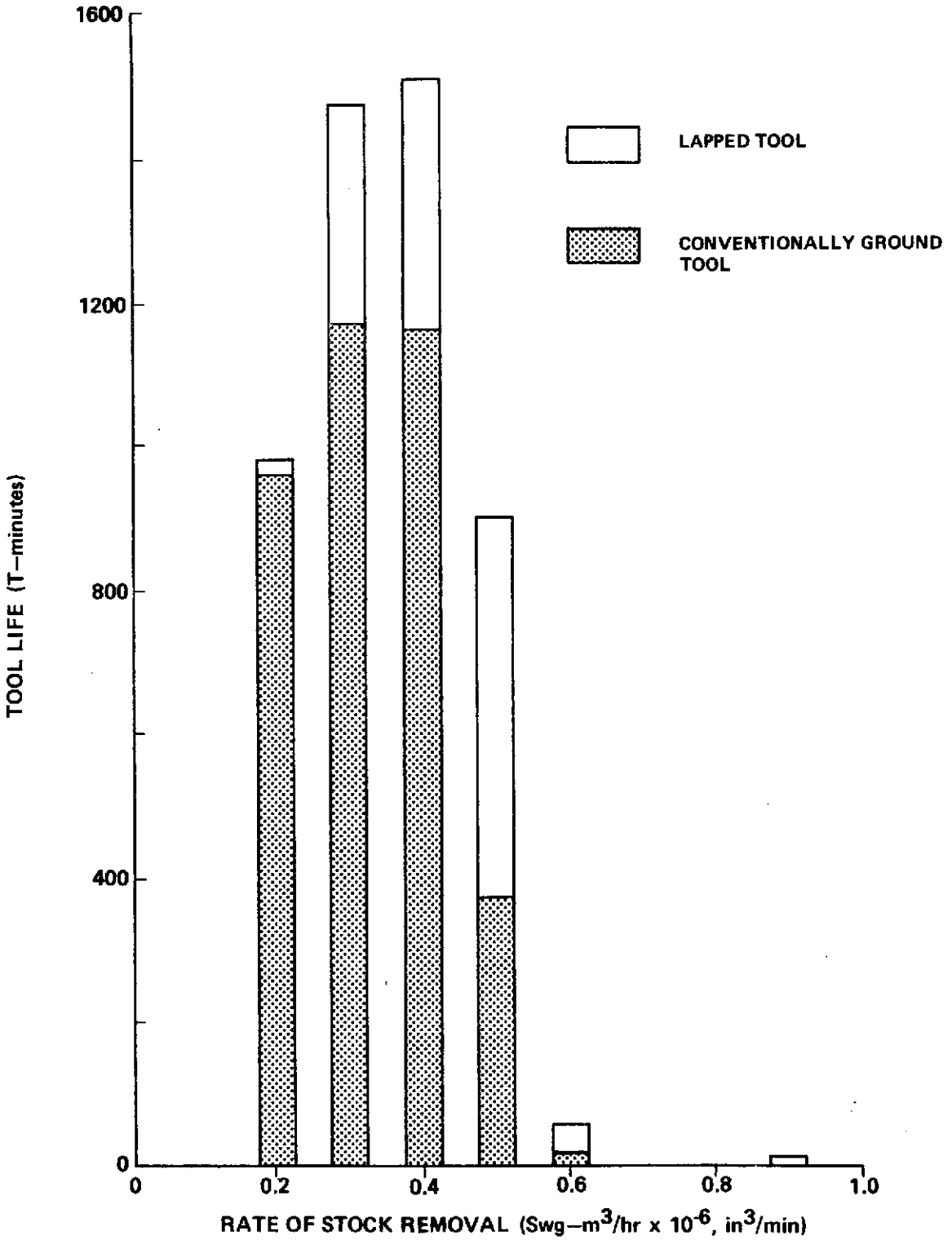

Figure 27. The variation of tool life with rate of stock removal comparing conventionally ground tooling with lapped tooling.

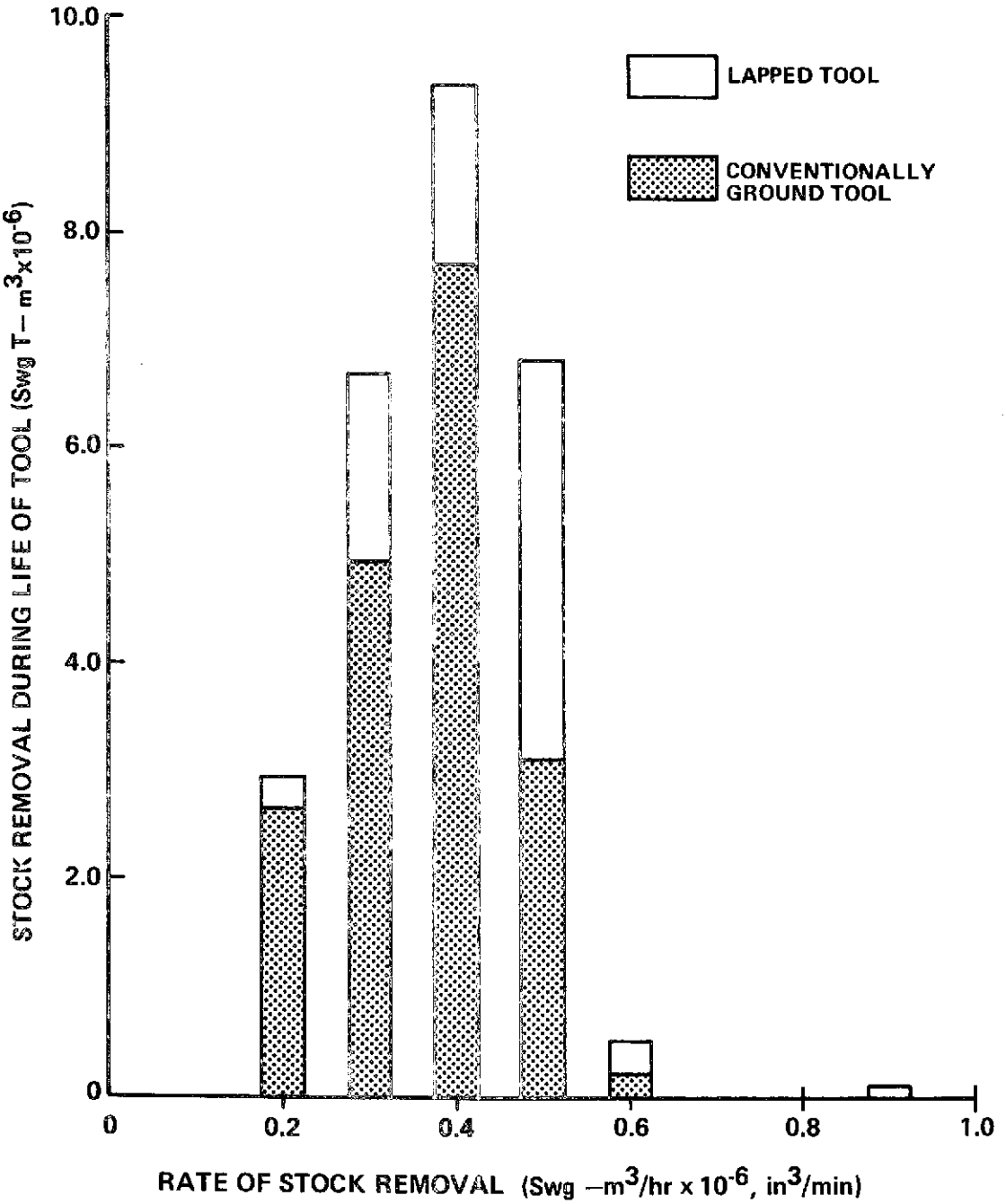

Figure 28. The variation of stock removed during the life of the tool with the rate of stock removal — when machining titanium.

The increased tool life us not quite so marked and is partly a function of reduced initial tool wear. However, a 30 percent increase in tool life is certainly beneficial, as the lapping principle described earlier will add very little to the cost of the tool.

One interesting outcome of the tool life tests described in this section is that tool life decreases as metal removal rates decrease (Fig. 27). This is opposite to what is generally found for more conventional materials.

The tool breakdowns at higher metal removal rates when machining titanium are almost certainly due to the increased cutting temperature due to unusually high chip velocities and low chip contact areas.

The decreased tool life at lower metal removal rates is not clearly understood, but may be due to the material work hardening more rapidly at reduced chip areas.

Whatever the reason, there is definitely an optimum metal removal rate for machining titanium, which is a feed of 0.19 mm/rev. and speed of 42 m/min., when machining without coolant.

The effectiveness of various coolants when machining titanium will be examined in the next section.

I. The Effectiveness of Different Coolant Techniques in Reducing Tool Temperature

1. Experimental Apparatus and Monitoring Equipment. A number of methods exist for measuring tool tip temperatures during machining. These are discussed by Cook [28], where he concludes that the tool-chip thermocouple is the best technique developed so far. In this work, however, where the comparison of different coolants is the objective, it was not necessary to determine an absolute value for tool tip temperature. Instead, the temperature was measured at three discrete points, 8.2mm, 14.0mm, and 19.7mm from the tool tip, on a line towards the center of the tool using Chromel-Alumel thermocouples. The thermocouples outputs were connected to a Brush, Mark 200, 8 channel pen recorder, using a 150°F reference junction.

The temperatures were allowed to stabilize for each machining test, so that the steady-state temperature profile of the test could be obtained. The temperature profile when machining with coolant would be compared with the temperature profile obtained when machining dry so that the temperature drop due to the particular coolant technique could be determined. The temperature drop for different coolants would then be compared.

H.S.S. Tooling was used for these tests with the following tool geometry:

Side rake	=	10 deg
Back rake	=	10 deg
End relief	=	3 deg
End clearance	=	8 deg
Side relief	=	3 deg
Side Clearance	=	8 deg
Side cutting edge	=	3 deg
End cutting edge	=	10 deg
Nose radius	=	0.25mm

2. Results. The temperature drop relative to dry machining is plotted against the distance from the tool tip in Figure 29. The steady-state temperature profile above ambient, when dry machining, is also plotted as an indication of the levels of cooling obtained.

It can be seen that spray mist cooling with 100 psi air pressure gives the most cooling, reducing the tool temperature to below their initial ambient condition. Lowering the spray mist air pressure to 30 psi, however, severely limited the amount of cooling to below that obtained with flood coolant. The through-the-tool coolant technique gave very little cooling, even less than holding an air jet to the tool. The poor results may be because the coolant channels within the tool end were 19mm (0.75 in.) from the tool tip.

One coolant technique tested, but not illustrated, was a modern form of the Hilsch tube which divides an air stream into a cold stream and a hot stream. Connecting the cold end to the spraymist applicator gave encouraging results, but lacked the cold air pressure to improve on the regular spray mist technique.

Finally, flank wear land is plotted against time in Figure 30 where the results for no coolant, spray mist, and flood coolant are compared. Whereas, there is no significant difference between the flood coolant and spray mist, the result does demonstrate that tool life can be extended by at least a factor of three by using one of these two techniques.

3. Discussion of Results. It has been shown in this section that either spray mist or flood coolant can be used to extend the maximum cutting speed when machining titanium. It is shown for a cutting speed of 54 m/min., that tool life can be extended by a factor of three using these coolants.

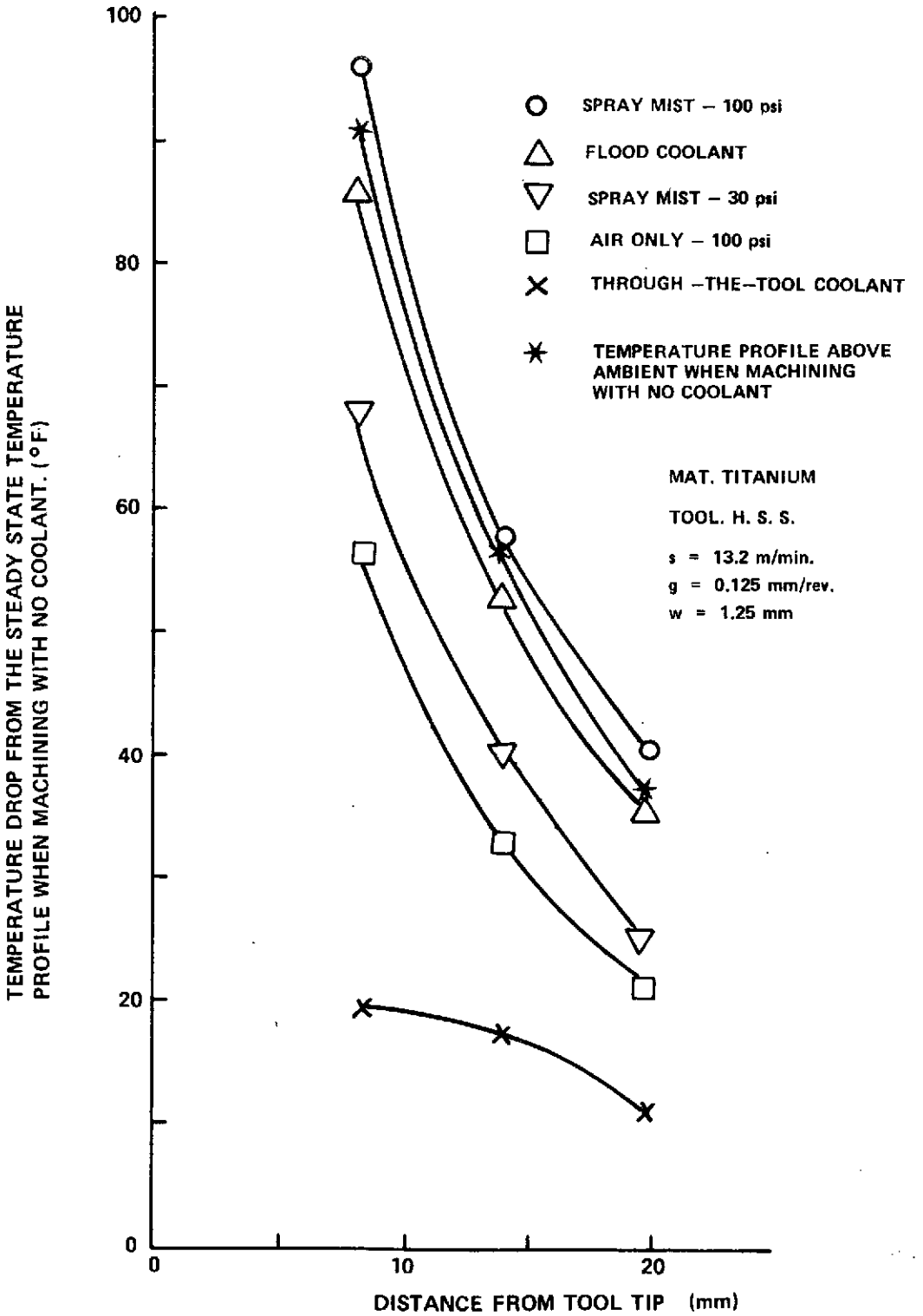

Figure 29. Temperature drop with distance from tool tip for different coolant techniques.

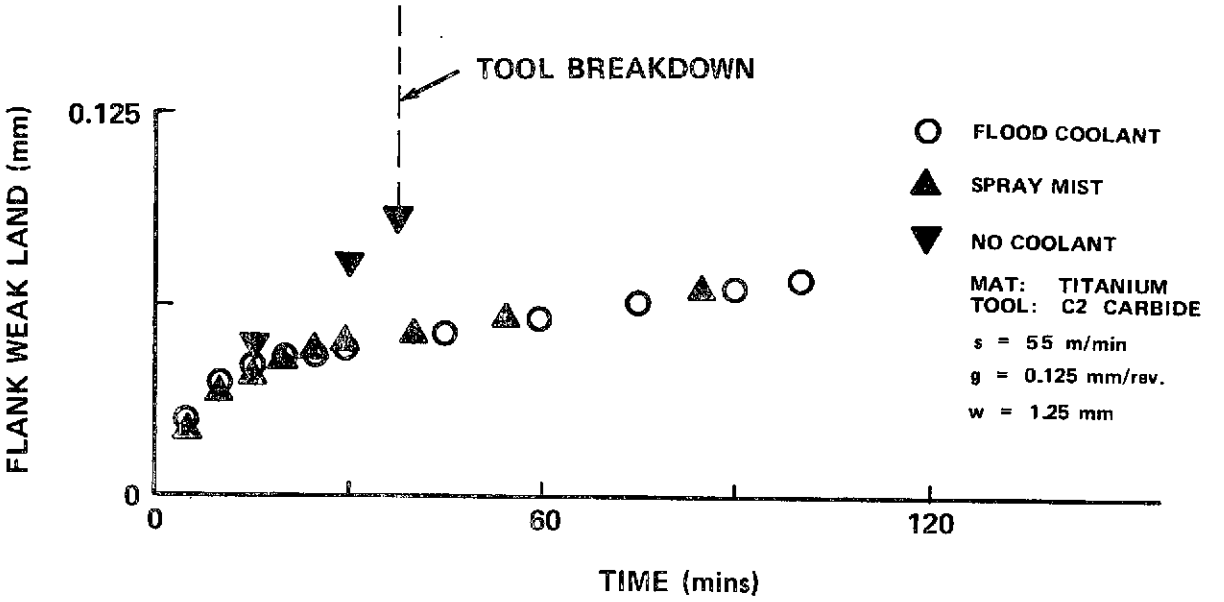

Figure 30. Flank wear land against time curves, with and without coolant.

Kececioglu and Sorensen [29] have shown that the tool life benefits obtained when using spray mist rather than flood coolant, and machining SAE 1045 steel, are dependent on cutting speed and whether land or crater wear is used as the wear criterion. These variations with speed might well exist when machining titanium. Because of this, no final conclusion can be made from these results on the relative merits of these two coolants when machining titanium for machining speeds other than those tested.

It is suggested that the optimum speed of 42 m/min and feed of 0.19 mm/rev., recommended in the previous section , can be extended when the above coolants are used.

SECTION III. CONCLUSIONS

The static cutting tests demonstrate that there are both tool nose forces and components of the cutting force in the thrust direction that deflect the cutting tool and result in poor machining tolerances. The tool nose forces are found to be particularly large when machining titanium compared to a free machining material. It is demonstrated that the cutting force component in the thrust direction can be minimized by the choice of the tool rake angle and that the tool nose forces can be significantly reduced by lapping the tool after grinding it.

The dynamic cutting tests demonstrate that the dynamic cutting force in the thrust direction due to flank contact is a quadrature stabilizing force, inversely proportional to the cutting speed, inversely proportional to flank clearance angle, proportional to the square of flank land, and a function of the metal cutting process. The workpiece material is only found to affect the magnitude of this stabilizing force. Productivity therefore can be increased, without incurring chatter problems, by using simple tool grinding procedures.

The tool finish tests show that improving tool finish reduces machining tolerances and increases tool life. Optimum machining conditions are recommended for machining titanium with lapped and as-ground tools, with tool life reducing at low and high machining speeds. Spray mist coolant is demonstrated to be most effective when machining titanium, increasing tool life by more than three times compared to machining without coolant.

APPENDIX

Titanium is a low-density, silver white metal and is important due to a combination of its lightness, strength and corrosion resistance. With a density half-way between that of aluminum and that of steel, titanium alloys are usually much stronger than aluminum alloys and have a tensile strength and hardness approaching that of many steels. Titanium alloys have a strength-to-weight ratio exceeding that of either aluminum or stainless steel between 400°F and 800°F. They also have good impact strength and resistance to fatigue. Titanium is more inert than aluminum and has better corrosive resistance to sea water than stainless steel. The chief disadvantages are high cost, difficulties in fabrication, and excessive reactivity at temperatures in excess of 1000°F. [30].

Although the element titanium was discovered by William Gregor in 1790, over 100 years passed before it was put to commercial use, and then only as an alloy additive to iron and steel. Titanium metal has been produced commercially only since 1948, and it was not till the introduction of the Kroll process a few years later that titanium production really became competitive. With the steady increase in demand for titanium over the last twenty years, the price has dropped from $10.90/lb in 1953 to $3.50/lb today, despite increasing inflation.

The latest titanium statistics [31] show that 81 percent of the titanium metal produced in the United States is for aerospace application, of which 40 percent is used for aircraft turbine engines, 36 percent is used for commercial and industry airframes and 5 percent is used for missile and space applications. There are about 30 commercially available grades of pure titanium and alloys, but an alloy containing 6 percent aluminum and 4 percent vanadium (Ti-6Al-4V) comprises 56 percent of the total mill products used. Ti-6Al-4V alloys are used extensively for both structural and rotating parts in the compressor section of turbine engines used in modern high performance military and civilian aircraft, and include such components as turbine compression blades, engine cases, frames, struts and forgings. Titanium is used in airframe structures, replacing aluminum and steel to reduce the weight of selected parts such as frames, bulkheads, hangers, skins, fasteners, firewalls, ducting, tubing, forgings, landing gear assemblies and in particular for parts subjected to elevated temperature. Whereas aircraft certified in the mid-1960's utilized titanium for up to 3 percent of the total structural weight, highly efficient military aircraft such as the A-11 and projected supersonic transports were

designed to contain up to 90 percent titanium. There is even an increase in the use of titanium for modern civilian supersonic aircraft. Whereas only 500 pounds of titanium is used in each Boeing 707, there is 18,000 pounds (9.2 percent of body weight) used in each Boeing 747 [31,32].

The Space Industry also is a major user of titanium and is liable to increase its usage as the trend toward reusable space hardware continues. Even in past programs, titanium has been widely used. The Mercury Spacecraft used in the United States first manned orbital flight was made principally of titanium. Titanium also was used extensively in the Gemini two-man and the Apollo three-man spacecraft. The pressurized compartment for the crew, various pressure vessels, and the solid-fuel cases for the retro-rockets in the spacecraft were made mostly of titanium and its alloys. Storage tank systems and other components of titanium were utilized in the Lunar Excursion Modules. Future programs, such as the Shuttle program, plan to use the alloy Ti-6A1-4V for the upper and lower main engine thrust structure, the elevons, and the pressure vessels of the orbiter.

The increase in usage of titanium in the aerospace industry is, in general, a good measure of the increased amount of titanium machining. This is particularly true for turbine engine components, high load carrying structural members, landing gear, engine frameworks and parts subjected to elevated temperature. Components such as skins, tubing and welded structures, in general, require little maching. The bulk of titanium components, therefore, require machining and, with designers becoming increasingly aware of the advantages and uses of titanium (even in non-aerospace applications), there will be a similar awareness towards increasing its machinability.

REFERENCES

1. American Society for Metals: Machining Difficult Alloys. Reinhold, New York Pub. Corp., 1962.

2. Wilson, F.W., and Cox, R.W., ed.: Machining the Space Age Metals. Am. Soc. of Tool and Manufacturing Engrs., Detroit, Mich., 1965.

3. Field, M.: Machining Aerospace Alloys. ISI Proceedings, Conference on Machineability, London, (1965), 1967, pp. 151-160; Discussion pp. 163-169.

4. Shaw, M.C.; and Nakayama, K.: Machining High Strength Materials. Annals of the CIRP, Vol. 15, No. 1, June 1967, pp. 45-59.

5. Sisson, T.R.; and Kegg, R.L.: An Explanation of Low Speed Chatter Effects. Trans. ASME, J. of Engrg. for Ind., Nov. 1969, pp. 951-958.

6. Merchant, M.E.: Mechanics of the Metal Cutting Process. J. Appl. Phys., 1954, vol. 16, nos. 5 and 6, pp. 268, 318.

7. Hsü, T.C.: An Analysis of the Plastic Deformation Due To Orthogonal and Oblique Cutting. J. Strain Analysis, 1966, vol. 1, p. 375.

8. Fenton, R.G.; and Oxley, P.L.B.: Mechanics of Orthogonal Machining - Predicting Chip Geometry and Cutting Forces From Work Material Properties and Cutting Conditions. Proc. Inst. Mech. Engrs. (London), 1969-70, Vol. 184, Pt. 1, No. 49, p. 927.

9. Albrecht, P.: New Developments in the Theory of Metal Cutting Process: The Ploughing Process in Metal Cutting, Trans., ASME, 1960, vol. 82, Series B, p. 348.

10. Wallace, P.W.; and Boothroyd, G.: Tool Forces and Tool-Chip Friction in Orthogonal Machining. JMES, 1964, Vol. 6, No. 1, p. 74.

11. Bailey, J.A.; and Boothroyd, G.: Critical Review of Some Previous Work on the Mechanics of the Metal Cutting Process. Trans. ASME, 1968, vol. 90(B), p. 54.

REFERENCES (Continued)

12. Wallace, P.W.; and Andrew, C.: Machining Forces: Some Effects of Tool Vibration. JMES, vol. 7, no. 2, 1965, p. 152.

13. Kegg, R.L.: Chatter Behavior at Low Cutting Speeds. Presented at the 18th Gen. Assembly of C.I.R.P., Great Britain, Sept. 1968.

14. Stewart, V.A.: The Mechanics of Continuous Chip Formation Under Regenerative Chatter Conditions. Ph.D. thesis, Monash University, Australia, 1971.

15. Tobias, S.A.: Machine-Tool Vibration. John Wiley and Sons, Inc., 1965, pp. 146-179, 270-273.

16. Sutherland, I.A.: The Development of a Two Component Force Dynamometer and Tool Control System for Dynamic Machine Tool Research. NASA TMX-64786, 1973.

17. Takeyama, H.; and Usui, E.: Effect of Tool-Chip Contact in Machining. Trans. ASME, 1958, vol. 80, p. 1089.

18. Sutherland, I.A.; and Andrew, C.: Forced Vibration and Chatter in Horizontal Milling: An Investigation Using a Structural Model. Proc. Instn. Mech. Engrs. (London), 1968-9, vol. 183 (Pt. 1, no. 31), pp. 395-416.

19. Smith, S.D.; and Tobias, S.A.: The Dynamic Cutting of Metals. Int. J. Mech. Tool Des. Res., vol. 1, 1961, pp. 283-292.

20. Wicher, A.; and Pape, R.: Formation of Oxide Layers on Cemented Carbide Tools During the Machining of Steel. Stahl und Eisen, Vol. 87, No. 20, October 5, 1967, pp. 1169-1178.

21. Stanislao, J.; Richman, M.H.; and James C.F.: The Effect of the Titanium Carbide Content of Cemented WC — TiC Cutting Tools in the Machining of Steels and Cast Irons. Journal of Materials, vol. 2, Sept. 1967, pp. 625-637.

REFERENCES (Concluded)

22. Ljungquist, R.: Development of Titanium-Carbide Coated Cemented Carbide Inserts. Proceedings of the Third International Conference on Chemical Vapor Deposition, Salt Lake City, Utah, April 24-27, 1972, pp. 383-396.

23. Mayer, J.E.; and Cowell, S.: Cemented Titanium Carbide Cutting Tools — Performance of Finishing, Semi-Finishing and Roughing Grades. Society of Manufacturing Engineers, Paper No. MR71-934, 1971.

24. Suh, N.P.; Shyam, S.; and Naik, S.K.: Enhancement of Tungsten-Carbide Tool Life by Oxide Treatment. Journal of Engineering for Industry, Trans., ASME, Series B, Vol. 94, Nov. 1972, pp. 979-984.

25. Kane, G.E.; and Zimmers, E.W., Jr.: The Influence of Preparation of Cutting Tools upon Their Performance. ASTME, Paper No. MR68-171, Vol. 68, No. 1, April 29-May 3, 1968.

26. Montag, G.; and Lierath, F.: The Wear and Tool Life Behavior of Carbide Tools Ground by Difference Processes. Fertigunstech Betrieb (in German), No. 9, Sept. 1967, pp. 534-538.

27. Abernathy, W.J.: Abrasive Articles and Methods of Making Abrasive Articles. U.S. Patent No. 3287861/2, Nov. 1966.

28. Cook, N.H.: Manufacturing Analysis. Addison Wesley, 1966, pp. 44-53.

29. Kececioglu, D.; and Sorensen, A.S.: Comparative Effect of Land and Crater Wear on Tool Life When Dry Cutting, Mist Cooling, and Flood Cooling. Trans. ASME, J. of Engrg. for Industry, Feb. 1962, vol. 84, Series B, pp. 49-52.

30. U.S. Bureau of Mines: Minerals, Facts and Problems. 1970 (Washington), pp. 773-794.

31. Kessler, H.D., Vice President of Materials Engineering, Reactive Metals, Niles, Ohio: Private Communication. Sept. 1973.

32. Tarasov, L.P.: The Future of Titanium. Machinery and Production Engineering, April 8, 1970, p. 533.

APPROVAL

AN INVESTIGATION OF CHATTER AND TOOL WEAR WHEN MACHINING TITANIUM

By Ian A. Sutherland

The information in this report has been reviewed for security classification. Review of any information concerning Department of Defense or Atomic Energy Commission programs has been made by the MSFC Security Classification Officer. This report, in its entirety, has been determined to be unclassified.

This document has also been reviewed and approved for technical accuracy.

DR. M. P. SIEBEL
Director, Process Engineering Laboratory